



RESEARCH MEMORANDUM

INVESTIGATION OF EXTENSIBLE WING-TIP AILERONS ON AN
UNTAPERED SEMISPAN WING AT 0° AND 45° SWEEPBACK

By John R. Hagerman and William M. O'Hare

Langley Aeronautical Laboratory
Langley Air Force Base, Va.

CLASSIFICATION CANCELLED

CLASSIFIED DOCUMENT

This document contains classified information affecting the National Defense of the United States within the meaning of the Espionage Act, U.S.C. 561 and 562. Its transmission or the revelation of its contents in any manner to an unauthorized person is prohibited by law. Information so classified may be imparted only to persons in the military and naval services of the United States, appropriate civilian officers and employees of the Federal Government who have a legitimate interest therein and to United States citizens of known loyalty and discretion who of necessity must be informed thereof.

Authority NACA R 7-2454 Date 8/18/54

By MTA 9/8/54 See

NATIONAL ADVISORY COMMITTEE FOR AERONAUTICS

WASHINGTON
September 20, 1949

UNCLASSIFIED



UNCLASSIFIED

NATIONAL ADVISORY COMMITTEE FOR AERONAUTICS

RESEARCH MEMORANDUM

INVESTIGATION OF EXTENSIBLE WING-TIP AILERONS ON AN
UNTAPERED SEMISPAN WING AT 0° AND 45° SWEEPBACK

By John R. Hagerman and William M. O'Hare

SUMMARY

A low-speed wind-tunnel investigation was made to determine the lateral control characteristics of extensible wing-tip ailerons on an untapered semispan wing having two configurations; one configuration was unswept and had an aspect ratio of 3.13 and the other configuration was swept back 45° and had an aspect ratio of 1.59. Three plan forms of extensible ailerons were investigated on each wing configuration at various amounts of extension and deflection relative to the wing-chord plane. Also, wing aerodynamic characteristics were determined for the two plain-wing configurations.

The results indicate that sufficient aileron effectiveness was generally obtained at moderate and high lift coefficients with the extensible ailerons investigated. However, the control effectiveness at low lift coefficients appears to be inadequate for satisfactory application to an airplane. It is thought that the extensible ailerons may be sufficiently effective for some types of missiles.

Yawing moments produced by the extensible ailerons investigated were comparable to those produced by conventional flap-type ailerons.

INTRODUCTION

The National Advisory Committee for Aeronautics is currently investigating the lateral-control problem associated with transonic and supersonic wing configurations. Because conventional flap-type ailerons do not always provide adequate lateral control throughout the speed range, particularly above the wing critical speed, other lateral-control devices are being investigated. Among the lateral-control devices being investigated are extensible wing-tip ailerons.

UNCLASSIFIED

These ailerons can be utilized in various ways - such as, by extending the aileron at a given deflection from one wing tip, or extension and deflection of one aileron on one wing tip. One of the important advantages to be derived from the use of these ailerons is that they would allow use of full-span high-lift flaps to alleviate somewhat the problem presented by the excessive speeds required for take-off and encountered in landing of airplanes having high wing loadings. Another advantage gained from the use of extensible wing-tip ailerons is the reduction of the problem concerning large operating forces at high speeds associated with flap-type ailerons.

Very little aerodynamic data pertaining to extensible wing-tip ailerons are available. However, reference 1 reports a low-speed investigation of this type of aileron on a rectangular wing of higher aspect ratio than that used in the present investigation and shows that rolling moment increases approximately linearly with aileron extension and also increases with increase in wing lift coefficient.

The present low-speed investigation, performed in the Langley 300 MPH 7- by 10-foot tunnel, was made to determine if adequate aileron effectiveness at low lift coefficients could be obtained for extensible wing-tip ailerons without resorting to simultaneous extension and deflection of the aileron. Two untapered high-speed wing configurations were used: one wing configuration was unswept and had an aspect ratio of 3.13; the other configuration, obtained by sweeping the unswept wing about the 50-percent root-chord station, was swept back 45° and had an aspect ratio of 1.59. A large-chord parallelogram aileron, a triangular aileron, and a short-chord parallelogram aileron were tested at various amounts of extension and deflection with respect to each wing configuration through a large angle-of-attack range.

COEFFICIENTS AND SYMBOLS

The forces and moments measured on the two wing configurations are presented about the wind axes, which, for the conditions of these tests (zero yaw), correspond to the stability axes. The X-axis is in the plane of symmetry of each model configuration and is parallel to the tunnel air flow. The Z-axis is in the plane of symmetry of each model configuration and is perpendicular to the X-axis. The Y-axis is mutually perpendicular to the X-axis and Z-axis. The three axes intersect in the plane of symmetry at the quarter chord of the mean aerodynamic chord of each configuration (figs. 1 and 2).

The symbols used are as follows:

- C_L lift coefficient $\left(\frac{\text{Twice lift of semispan model}}{qS} \right)$
- $C_{L_{\max}}$ maximum lift coefficient
- C_D drag coefficient (D/qS)
- C_M pitching-moment coefficient
 $\left(\frac{\text{Twice pitching moment of semispan model about Y-axis}}{qS\bar{c}} \right)$
- C_l rolling-moment coefficient (L/qSb)
- C_n yawing-moment coefficient (N/qSb)
- $C_{L_\alpha} = \frac{\partial C_L}{\partial \alpha}$
- C_{l_p} damping-in-roll coefficient; that is, rate of change of rolling-moment coefficient with wing-tip helix angle
 $\left(\frac{\partial C_l}{\partial \frac{pb}{2V}} \right)$
- $C_{n_p} = \frac{\partial C_n}{\partial \frac{pb}{2V}}$
- $pb/2V$ wing-tip helix angle, radians (C_l/C_{l_p})
- D twice drag of semispan model, pounds
- L rolling moment about X-axis due to one aileron extended and deflected, foot-pounds
- N yawing moment about Z-axis due to one aileron extended and deflected, foot-pounds
- c local wing chord
- \bar{c} wing mean aerodynamic chord, 2.48 feet for unswept wing configuration and 3.52 feet for sweptback wing configuration
 $\left(\frac{2}{S} \int_0^{b/2} c^2 dy \right)$

| | |
|----------------|---|
| y | lateral distance from plane of symmetry, feet |
| S | twice area of semispan model, 19.16 square feet for unswept wing configuration and 19.32 square feet for sweptback wing configuration |
| S _a | aileron area, square feet (see table I) |
| b | twice span of semispan model, 7.75 feet for unswept wing configuration and 5.55 feet for sweptback wing configuration |
| b _a | aileron span, feet (see table I) |
| q | free-stream dynamic pressure, pounds per square foot ($\frac{1}{2}\rho V^2$) |
| V | free-stream velocity, feet per second |
| ρ | mass density of air, slugs per cubic foot |
| α | angle of attack with respect to wing-chord plane, degrees |
| δ _a | aileron deflection relative to wing-chord plane (positive when trailing edge is down), degrees |
| R | Reynolds number |
| M | Mach number (V/a) |
| a | speed of sound |

CORRECTIONS

The lift, drag, and pitching-moment-coefficient data presented herein are for a complete-wing model, and the lateral-control data represent the aerodynamic moments on a complete wing as a result of extending the aileron on one semispan wing of a complete-wing model.

Jet-boundary (induced upwash) corrections were applied to the angle-of-attack and drag values as outlined in reference 2. Blockage corrections were applied to the test data by the methods of reference 3.

Reflection-plane corrections were not applied to rolling-moment and yawing-moment coefficients because available correction data did not apply to the configurations of this investigation. However, by

extrapolation of data given in reference 4, it is estimated that the values of rolling-moment coefficient obtained were approximately 10 percent too high for both wings. Also, it is thought that the yawing moments, if corrected, would be more adverse than the data show.

MODEL AND APPARATUS

The two configurations of the semispan-wing model were mounted vertically in the Langley 300 MPH 7- by 10-foot tunnel as illustrated in figure 3. The root chord of the model (for each configuration) was adjacent to the ceiling, the ceiling serving as a reflection plane. A small clearance between the model and ceiling prevented ceiling interference of measurements of all forces and moments acting on the model. A fairing strip was attached to the root of the model to deflect air that flows into the tunnel through the clearance hole between the model and the tunnel ceiling, thus reducing the effect of the downflow on the regular flow over the model.

Both configurations of the semispan-wing model were untapered, had no twist or dihedral, and had NACA 64A010 airfoil sections normal to the leading edge. One configuration was unswept and had an aspect ratio of 3.13; the other configuration, obtained by sweeping the unswept wing about the 50-percent root-chord station, was swept back 45° and had an aspect ratio of 1.59. Dimensions of the two plan forms are given in figures 1 and 2. The model was equipped with full-span flaps which were locked at zero deflection during the present investigation. The extensible ailerons (figs. 1 and 2) consisted of a parallelogram and a triangular aileron with similar root chords (0.625c) and a parallelogram aileron with a chord of 0.156c and having an area about one-half as large as the other two ailerons. The trailing-edge sweep angle of each aileron was the same as the sweep angle of the corresponding wing configuration (figs. 1 and 2). The flat-plate type of ailerons was constructed of $\frac{1}{4}$ -inch sheet dural and had rounded leading edges and 12° beveled trailing edges along the entire span of each aileron. Table I presents the geometric characteristics of the extensible wing-tip ailerons.

Various extensions of each aileron were attached to the wing tip at the desired deflections with respect to the wing-chord plane with the brackets enclosed in a wing-tip fairing. The ailerons were deflected about a spanwise axis that passed through the 50-percent tip-chord station on each wing configuration except for several tests performed with the short-chord aileron deflected about a spanwise axis that passed through the 0.267 tip-chord station on the unswept wing

configuration (figs. 1 and 2). The aileron deflections were limited to a range that would enable the ailerons to remain within the wing contour when retracted at the given deflection.

TESTS

Lift tests were made through the angle-of-attack range from -6° to stall for the unswept and sweptback plain-wing configurations at Mach numbers of 0.19, 0.27, and 0.37. On the unswept wing, these Mach numbers correspond to Reynolds numbers of 3.2×10^6 , 4.5×10^6 , and 6.1×10^6 based on a mean aerodynamic chord of 2.48 feet; whereas, on the 45° sweptback wing, these Mach numbers correspond to Reynolds numbers of 4.5×10^6 , 6.3×10^6 , and 8.6×10^6 based on a mean aerodynamic chord of 3.52 feet.

Lateral-control data were obtained on the unswept and sweptback wing configurations through the angle-of-attack range from -6° to stall at an average dynamic pressure of approximately 51 pounds per square foot, which corresponds to a Mach number of 0.19. Aileron data were obtained for various combinations of aileron deflection and extension for each of the three ailerons on each of the two wing configurations.

DISCUSSION

Plain-Wing Aerodynamic Characteristics

The lift, drag, and pitching-moment characteristics of the unswept and 45° sweptback plain-wing configurations are shown in figures 4 and 5, respectively.

Unswept wing.— As Mach number and Reynolds number were increased, there was a slight increase in $C_{L\alpha}$ and a negligible change in drag and pitching-moment characteristics of the unswept wing for values of C_L below about 0.7 (fig. 4). The aerodynamic center of the unswept wing was about 4 percent mean aerodynamic chord ahead of the $\bar{c}/4$ over most of the angle-of-attack range; however, the wing had a stable stall region, a characteristic usually exhibited by low-aspect-ratio unswept wings.

The experimental value of $C_{L\alpha}$ of 0.055 measured for $M = 0.19$ is in excellent agreement with the value of 0.055 computed by the empirical method recommended in reference 5 but is lower than the

value of 0.059 computed by the theoretical method of reference 6 (using a value of 0.1075 for section lift-curve slope (reference 7)).

The lift curves for $M = 0.19$ and $M = 0.27$ indicate an increase in $C_{L_{max}}$ with an increase in Mach number and Reynolds number; however, an adverse compressibility effect at high lift coefficients, accompanied by a decrease in $C_{L_{max}}$, can be noted for $M = 0.37$. These effects correlate well with data from references 7 and 8 pertaining to Reynolds number and Mach number effects.

45° sweptback wing.— For the 45° sweptback wing configuration, $C_{L_{\alpha}}$ increased very slightly and the drag and pitching-moment characteristics changed negligibly as Mach number and Reynolds number were increased (fig. 5). The pitching-moment data for the sweptback wing indicate that the aerodynamic center was about 5 percent mean aerodynamic chord ahead of the $\bar{c}/4$ at low lift coefficients; however, at higher lift coefficients and through the stall region the wing was stable.

The experimental value of $C_{L_{\alpha}}$ obtained on the sweptback wing at $M = 0.19$ is 0.036. This value compares very well with similar values of $C_{L_{\alpha}}$ of 0.037 computed by the theoretical method of reference 6 (which accounts for sweep angle) and by the empirical method recommended in reference 5 (which considers aspect ratio as the only variable). This agreement between the estimated and measured values of $C_{L_{\alpha}}$ tends to substantiate the point made in reference 6 that sweep angle has little effect on $C_{L_{\alpha}}$ for wings of low aspect ratio.

The lift data for $M = 0.37$ were not obtained at lift coefficients high enough to observe any compressibility effect similar to that noted on the unswept wing configuration. However, the lift curves for $M = 0.19$ and $M = 0.27$ show a negligible change in $C_{L_{max}}$ with increase in Mach number and Reynolds number, possibly indicating the onset of adverse compressibility effects, or little effect of Reynolds numbers of 4.5×10^6 and 6.3×10^6 .

Comparison of the unswept and sweptback plain-wing configurations.— Comparison of the plain-wing aerodynamic data for the unswept and sweptback configurations shows that the results vary with aspect ratio and sweep angle as would be predicted by theory. The value of $C_{L_{\alpha}}$ was higher for the unswept configuration, primarily because of the higher aspect ratio of the unswept wing (reference 6). A larger value of $C_{L_{max}}$

was obtained on the sweptback configuration than on the unswept configuration, an effect which has been found previously in other investigations (for example, reference 9).

Drag coefficients of the sweptback wing were generally larger than those of the unswept wing, especially at large lift coefficients. Calculations indicate that this is accounted for mostly by the lower aspect ratio and the consequent larger values of induced drag of the sweptback wing. The maximum lift-drag ratio (which occurred at $C_L \approx 0.2$) was about 16 and 12 for the unswept and sweptback wing configurations, respectively.

The aerodynamic center was ahead of the $\bar{c}/4$ —approximately the same amount in percent mean aerodynamic chord at zero lift coefficient for both wing configurations. Both wing configurations exhibited stable stall characteristics; however, the unswept wing had a more nearly linear variation of c_m with α .

Lateral Control Characteristics

The rolling-moment and yawing-moment coefficients obtained for several extensions and deflections of the various plan forms of extendible wing-tip ailerons on the unswept wing configuration are shown in figures 6 to 11, and similar data obtained on the sweptback wing configuration are shown in figures 12 to 17. As previously discussed under the section entitled "Corrections," the rolling-moment and yawing-moment data presented in these figures are uncorrected for reflection-plane effects.

Unswept wing configuration.—The rolling-moment coefficients generally increased with increase in α for all aileron deflections and extensions on the unswept wing configuration.

The rolling-moment data indicate a reversal of direction of roll at some negative angles of attack, a highly undesirable condition for inverted flight and some maneuvers. Utilizing greater aileron deflections than those used in this investigation would probably relieve the undesirable condition somewhat since reversal of rolling moment occurs at larger negative angles of attack with increased aileron deflections.

Deflecting the large-chord and triangular ailerons caused fairly linear increases in rolling moment for the deflection-range tested (figs. 6 and 8). For the short-chord aileron, no appreciable increase in rolling moment was gained by deflecting the aileron beyond 4° at positive angles of attack, probably because of early separation over the aileron which was accentuated with increased deflection. However, the rolling moment produced by the short-chord aileron continued to

increase with increasing α even at the large aileron deflections, probably because as the wing continued to load up, mutual interference between the wing and the aileron (induction effects) tended to increase further the loading on the wing.

Except at some negative values of α , an increase of aileron extension at constant aileron deflection caused an increase in rolling moment for all angles of attack and for all aileron configurations (figs. 7, 9, and 11).

Several tests performed with the fully extended short-chord aileron moved forward on the wing so the aileron midchord would coincide with the 0.267c line of the unswept wing showed that the aileron produced approximately the same lateral control characteristics on the wing as when in the normal position investigated (fig. 10).

The short-chord aileron-wing configuration reported herein was geometrically comparable to the extensible wing-tip aileron described in reference 10, but comparison between the results of the two investigations was available for only $\alpha = 0^\circ$. Although larger values of C_l were obtained for various aileron extensions in the present case, both investigations showed the same general variation of rolling moment with aileron extension.

Comparing the three ailerons of this investigation on the basis of equal values of S_a/S , it can be noted that for similar aileron deflections each of the ailerons on the unswept wing configuration generally produced about the same amount of rolling moment, except at high angles of attack where the short-chord aileron did not produce rolling moments as great as those produced by the large-chord or triangular ailerons (figs. 7, 9, and 11).

The yawing moments produced by each of the aileron configurations were generally adverse over the entire α range and became more adverse with increase in α , aileron deflection, and/or aileron extension. The adverse C_n/C_l ratio was large for all aileron configurations at large angles of attack, but was largest for the short-chord aileron, being larger than 0.25.

45° sweptback wing.—As was the case of the unswept wing, the rolling moments produced by the various ailerons on the 45° swept wing generally increased with increase in α (figs. 12 to 17). The rolling-moment data show a reversal of roll direction at some negative angles of attack, as did the aileron on the unswept wing.

Deflecting each of the ailerons effected fairly linear increases in rolling moments at all positive angles of attack for the aileron-deflection range investigated (figs. 12, 14, and 16). Unit deflection

of the short-chord aileron produced larger incremental roll at low angles of attack than at high angles of attack (fig. 16). This phenomenon concerning the short-chord aileron was also noted on the unswept wing configuration and was attributed earlier in the paper to separation of flow over the aileron.

Except at some negative values of α , an increase of aileron extension at constant deflection for each aileron plan form caused an increase in rolling moment for all angles of attack (figs. 13, 15, and 17).

On the basis of equal values of S_a/S and at the same deflection, the short-chord aileron produced rolling moments over the entire α range comparable to the rolling moments produced by the large-chord and triangular ailerons (figs. 13, 15, and 17).

Adverse yawing moments were produced by the ailerons for all positive angles of attack, generally becoming more severe with increased α (figs. 12 to 17). Yawing moments also became more adverse with an increase of aileron deflection or extension. The adverse C_n/C_l ratio amounted to as much as 0.6 for some aileron configurations at large angles of attack near $C_{l_{max}}$.

Comparison of the unswept and sweptback wing configurations.-

Comparison of the lateral-control data for the unswept and sweptback wing configurations shows that the rolling moments produced by each of the ailerons generally exhibited similar variations with change in angle of attack, aileron extension, and/or aileron deflection.

For any given value of C_l the triangular aileron on the unswept wing configuration generally produced greater rolling moments than the corresponding triangular aileron on the sweptback configuration, whereas the large-chord and short-chord ailerons on the unswept wing configuration generally produced smaller rolling moments than the corresponding ailerons on the sweptback configurations. However, because the damping-in-roll coefficient C_{l_p} is smaller for the sweptback wing than for the unswept wing (primarily because of the smaller aspect ratio of the sweptback wing (reference 11)), the values of the wing-tip helix angle $pb/2V$ produced by each of the ailerons on the sweptback wing configuration were considerably greater than the values of $pb/2V$ produced by the respective ailerons on the unswept wing configuration.

In order to compare the rolling effectiveness of the various ailerons, the variation of wing-tip helix angle $pb/2V$ with lift coefficient, estimated for the unswept and sweptback wing configurations, is given in figures 18 and 19, respectively. Values of the damping-in-roll coefficient C_{l_p} used in computing $pb/2V$ were 0.27 and 0.13 for

the unswept and sweptback wing configurations, respectively, and were obtained from reference 11. These values of C_{Lp} pertain to low-speed data for the wing alone and do not account for the increase in aspect ratio resulting from extending the aileron. All values of $pb/2V$ are probably high since rolling due to sideslip, yawing, and wing twist were neglected.

Except for the short-chord aileron on the unswept wing, for which the values of $pb/2V$ are low over the entire C_L range, aileron effectiveness available at moderate and large lift coefficients with each of the ailerons investigated on both wing configurations (figs. 18 and 19) would easily satisfy requirements of reference 12. However, at small lift coefficients, aileron effectiveness appears to be inadequate for application to an airplane. It is thought that the extensible ailerons may be sufficiently effective for some types of missiles.

Adverse yawing moments produced by the ailerons on the unswept and sweptback configurations generally varied in the same manner with changes in angle of attack, aileron deflection, and/or aileron extension, but yawing moments were generally larger for the sweptback configurations. These yawing moments were comparable to those produced by conventional flap-type ailerons.

The rudder deflection required in a roll to correct for adverse yawing moments due to aileron extension and yawing moments due to rolling was computed for an assumed airplane utilizing the 45° sweptback wing with triangular tip ailerons. The vertical tail of the assumed airplane had 45° of sweepback, an aspect ratio of 1.0, an area of 0.15 of the wing area, a rudder chord of 0.25 of the vertical-tail chord, and a tail length of $2.5\bar{c}$. For sweptback wings, yawing moments due to roll C_{np} are adverse at low lift coefficients and favorable

(C_n same sign as C_l) at high lift coefficients (reference 13).

For $\frac{pb}{2V} = 0.15$ and $C_L = 0.5$ (fig. 19(b), 1/2 aileron extension) and $C_{np} = -0.04$ (reference 13), a rudder deflection of less than 10° would maintain a coordinated roll. At high lift coefficients rudder deflections would be small since the adverse yawing moments due to aileron extension are counteracted by the favorable yawing moments due to roll.

CONCLUSIONS

A low-speed wind-tunnel investigation, made to determine the lateral control characteristics of extensible wing-tip ailerons on an untapered semispan wing at 0° and 45° sweepback, led to the following conclusions:

1. Sufficient aileron effectiveness was generally obtained at moderate and high lift coefficients with the extensible ailerons investigated. However, the control effectiveness at low lift coefficients appears to be inadequate for satisfactory application to an airplane. It is thought that the extensible ailerons may be sufficiently effective for some types of missiles.

2. Yawing moments produced by the extensible ailerons investigated were comparable to those produced by conventional flap-type ailerons.

Langley Aeronautical Laboratory
National Advisory Committee for Aeronautics
Langley Air Force Base, Va.



REFERENCES

1. Regenscheit, B.: Versuche mit einem Flügelendquerruder an einem Rechteckflügel. UM Nr. 3219, Aerodynamische Versuchsanstalt Göttingen, Feb. 2, 1945.
2. Polhamus, Edward C.: Jet-Boundary-Induced-Upwash Velocities for Swept Reflection-Plane Models Mounted Vertically in 7- by 10-Foot, Closed, Rectangular Wind Tunnels. NACA TN 1752, 1948.
3. Herroit, John G.: Blockage Corrections for Three-Dimensional-Flow Closed-Throat Wind Tunnels, with Consideration of the Effect of Compressibility. NACA RM A7B28, 1947.
4. Swanson, Robert S., and Toll, Thomas A.: Jet-Boundary Corrections for Reflection-Plane Models in Rectangular Wind Tunnels. NACA Rep. 770, 1943.
5. Wood, K. D.: Aspect Ratio Corrections. Jour. Aero. Sci., vol. 10, no. 8, Oct. 1943, pp. 270-272.
6. Polhamus, Edward C.: A Simple Method of Estimating the Subsonic Lift and Damping in Roll of Sweptback Wings. NACA TN 1862, 1949.
7. Loftin, Laurence K., Jr.: Theoretical and Experimental Data for a Number of NACA 6A-Series Airfoil Sections. NACA TN 1368, 1947.
8. Abbott, Ira H., Von Doenhoff, Albert E., and Stivers, Louis S., Jr.: Summary of Airfoil Data. NACA Rep. 824, 1945.
9. Goodman, Alex, and Brewer, Jack D.: Investigation at Low Speeds of the Effect of Aspect Ratio and Sweep on Static and Yawing Stability Derivatives of Untapered Wings. NACA TN 1669, 1948.
10. Anon: Wind-Tunnel Tests of the K4Q-1 Airplane. Part IV - Aileron Effectiveness for Various Partial Extensions. TED No. TMB 2328. David Taylor Model Basin, U.S.N., Washington, D. C., July 29, 1946.
11. Toll, Thomas H., and Queijo, M. J.: Approximate Relations and Charts for Low-Speed Stability Derivatives of Swept Wings. NACA TN 1581, 1948.
12. Anon: Flying Qualities of Piloted Airplanes. U. S. Air Force Specification No. 1815-B, June 1, 1948.

13. Goodman, Alex, and Fisher, Lewis R.: Investigation at Low Speeds of the Effect of Aspect Ratio and Sweep on Rolling Stability Derivatives of Untapered Wings. NACA TN 1835, 1949.

CONFIDENTIAL

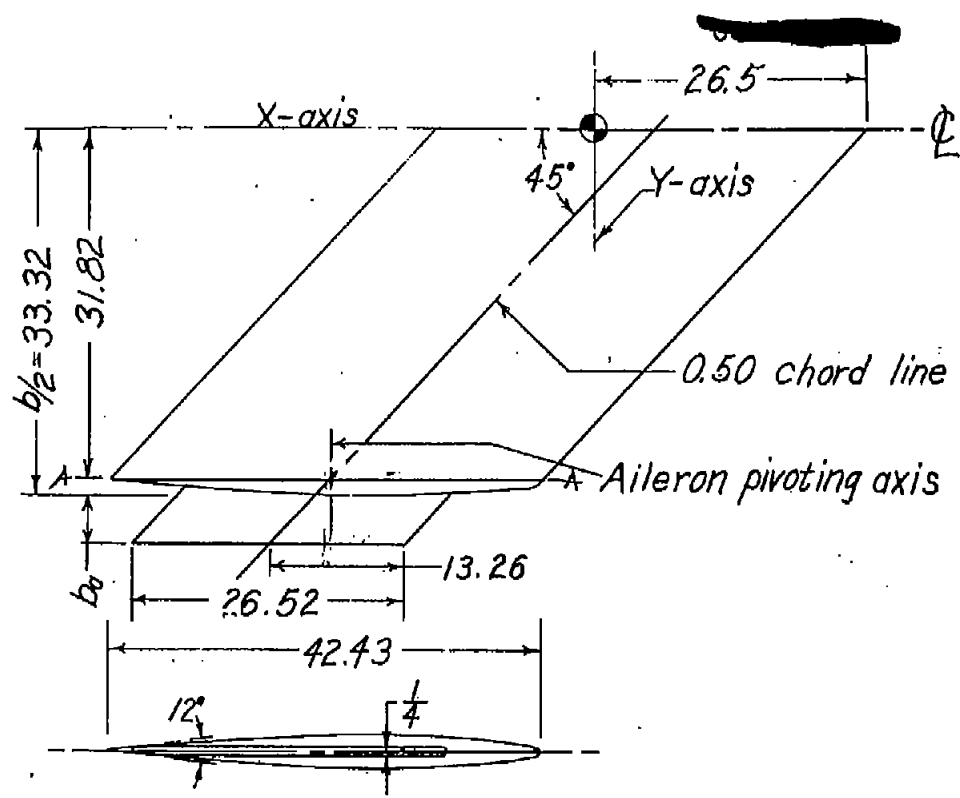
TABLE I
GEOMETRY OF THE EXTENSIBLE WING-TIP ALLERONS

| Aileron plan form | Aileron Extension | | | | Aileron chord | Aileron span Wing semispan, $\frac{b_a}{b/2}$ | | Aileron area, S_a (sq ft) | | Aileron area, $\frac{S_a}{S}$ Wing area | |
|-------------------|---------------------|----------------------|---------------------------------|----------------------|--------------------|--|----------------------|--------------------------------|----------------------|--|----------------------|
| | Nominal extension | | Actual extension, b_a (ft) | | | $\Lambda = 0^\circ$ | $\Lambda = 45^\circ$ | $\Lambda = 0^\circ$ | $\Lambda = 45^\circ$ | $\Lambda = 0^\circ$ | $\Lambda = 45^\circ$ |
| | $\Lambda = 0^\circ$ | $\Lambda = 45^\circ$ | $\Lambda = 0^\circ$ | $\Lambda = 45^\circ$ | | | | | | | |
| Large chord | Full | Full | 0.491 | 0.351 | 0.625 ^a | 0.127 | 0.126 | 0.766 | 0.775 | 0.040 | 0.040 |
| | 3/4 | 7/10 | .367 | .245 | | .095 | .083 | .573 | .542 | .030 | .028 |
| | 1/2 | 1/2 | .247 | .178 | | .064 | .064 | .386 | .393 | .020 | .020 |
| | 1/4 | 1/4 | .121 | .093 | | .031 | .033 | .189 | .206 | .010 | .011 |
| Triangular | Full | Full | .977 | .695 | .625 ^a | .252 | .250 | .764 | .767 | .040 | .040 |
| | 3/4 | 3/4 | .737 | .520 | | .190 | .187 | .576 | .574 | .030 | .030 |
| | 1/2 | 1/2 | .491 | .348 | | .127 | .125 | .384 | .384 | .020 | .020 |
| | 1/4 | 1/4 | .244 | .174 | | .063 | .063 | .191 | .192 | .010 | .010 |
| Short chord | Full | Full | 1.035 | .732 | .156 ^a | .267 | .263 | .402 | .402 | .021 | .021 |
| | 3/4 | 3/4 | .776 | .548 | | .200 | .197 | .302 | .302 | .016 | .016 |
| | 1/2 | 1/2 | .515 | .365 | | .133 | .131 | .200 | .201 | .011 | .011 |
| | 1/4 | 1/4 | .259 | .186 | | .067 | .067 | .101 | .102 | .005 | .005 |

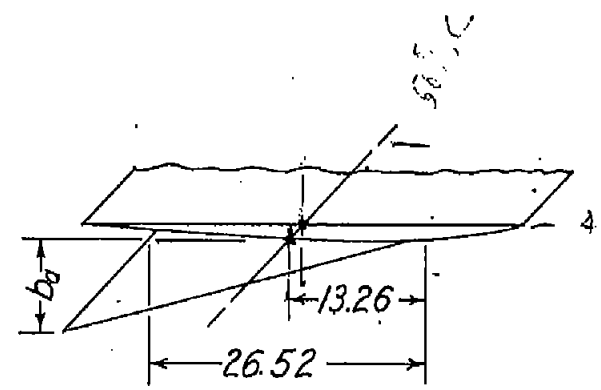
^aAt root chord of aileron.

CONFIDENTIAL

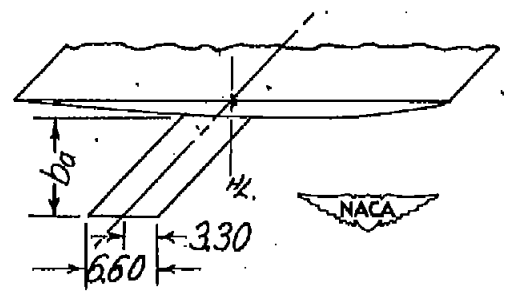




(a) Large-chord extensible aileron on wing.

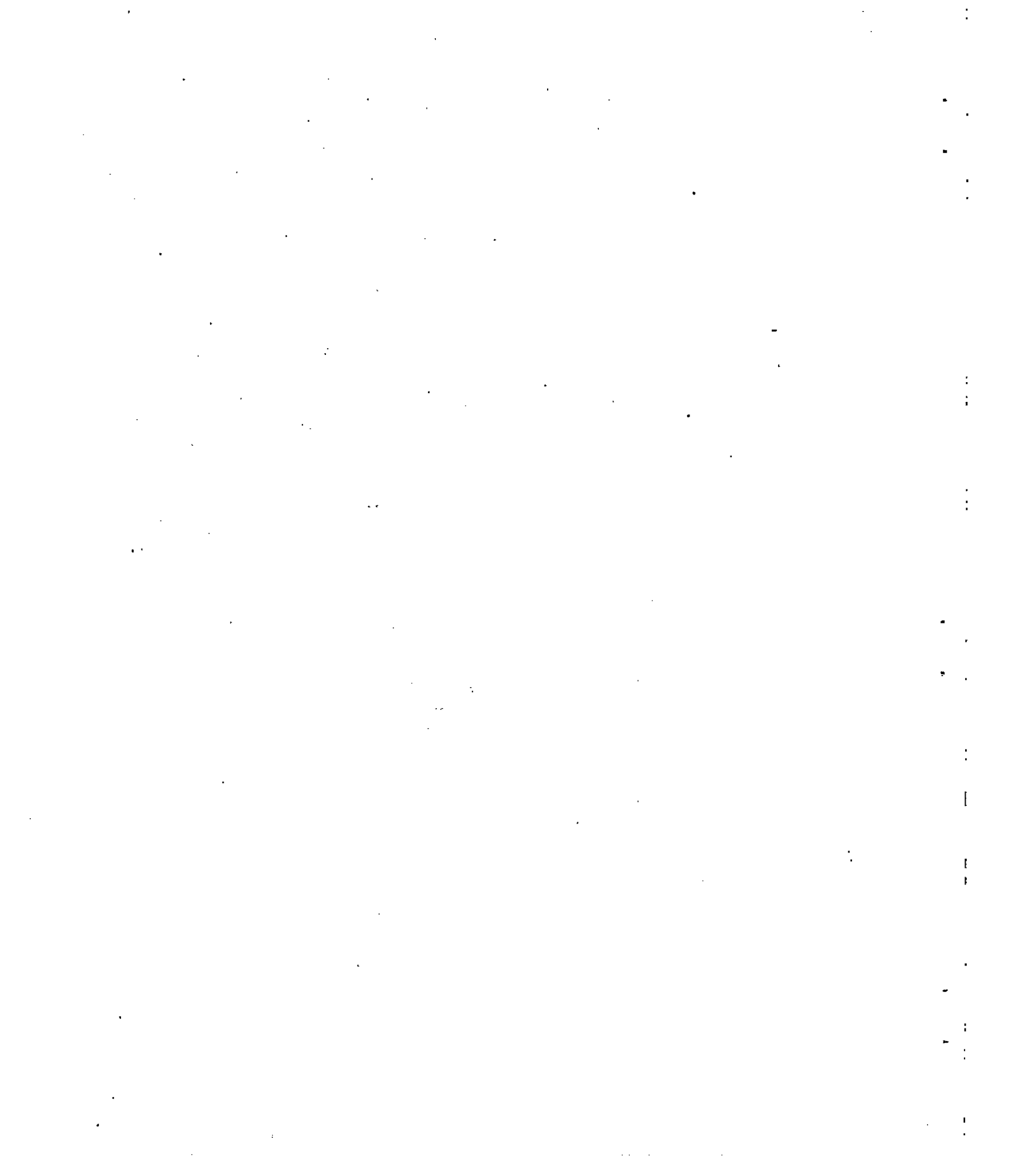


(b) Triangular extensible aileron on wing.



(c) Short-chord extensible aileron on wing.

Figure 2.- Schematic drawing of the 45° sweptback configuration of the untapered semispan-wing model and the extensible wing-tip ailerons. Wing area = 19.32 square feet; aspect ratio = 1.59. (All dimensions are in inches unless otherwise noted.)



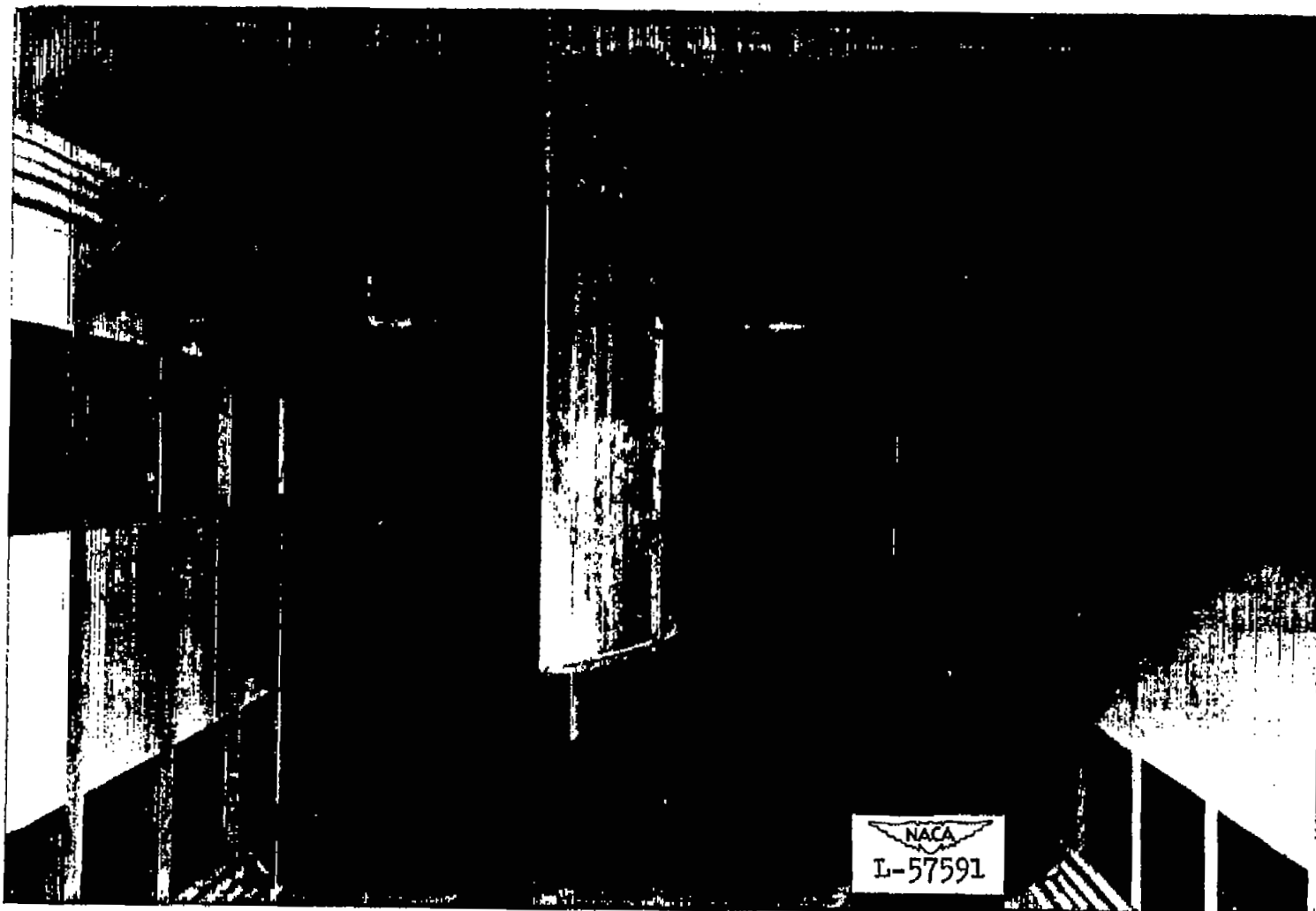
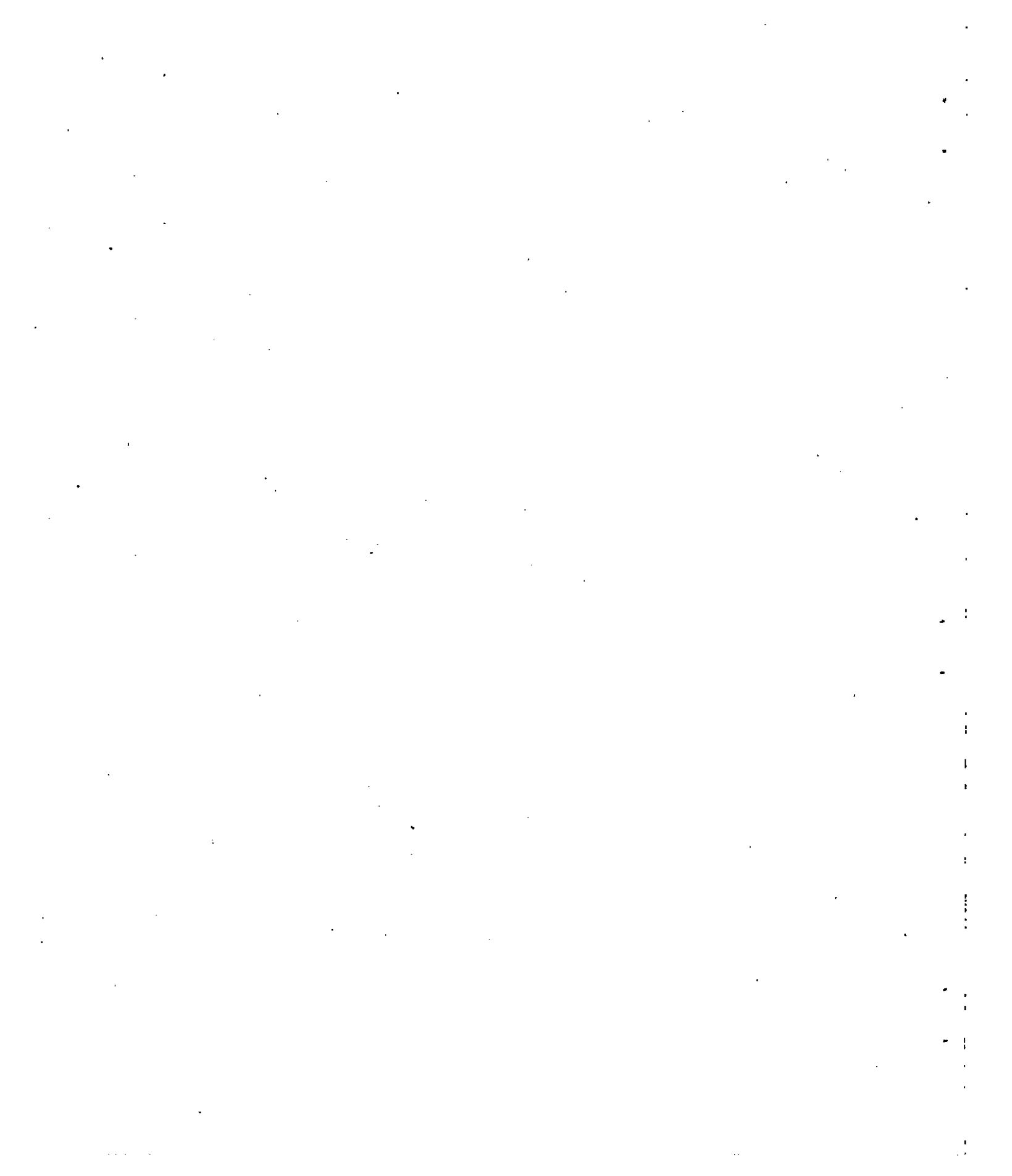


Figure 3.- The fully extended large-chord aileron attached to the unswept, untapered semispan wing configuration mounted in the Langley 300 MPH 7- by 10-foot tunnel.



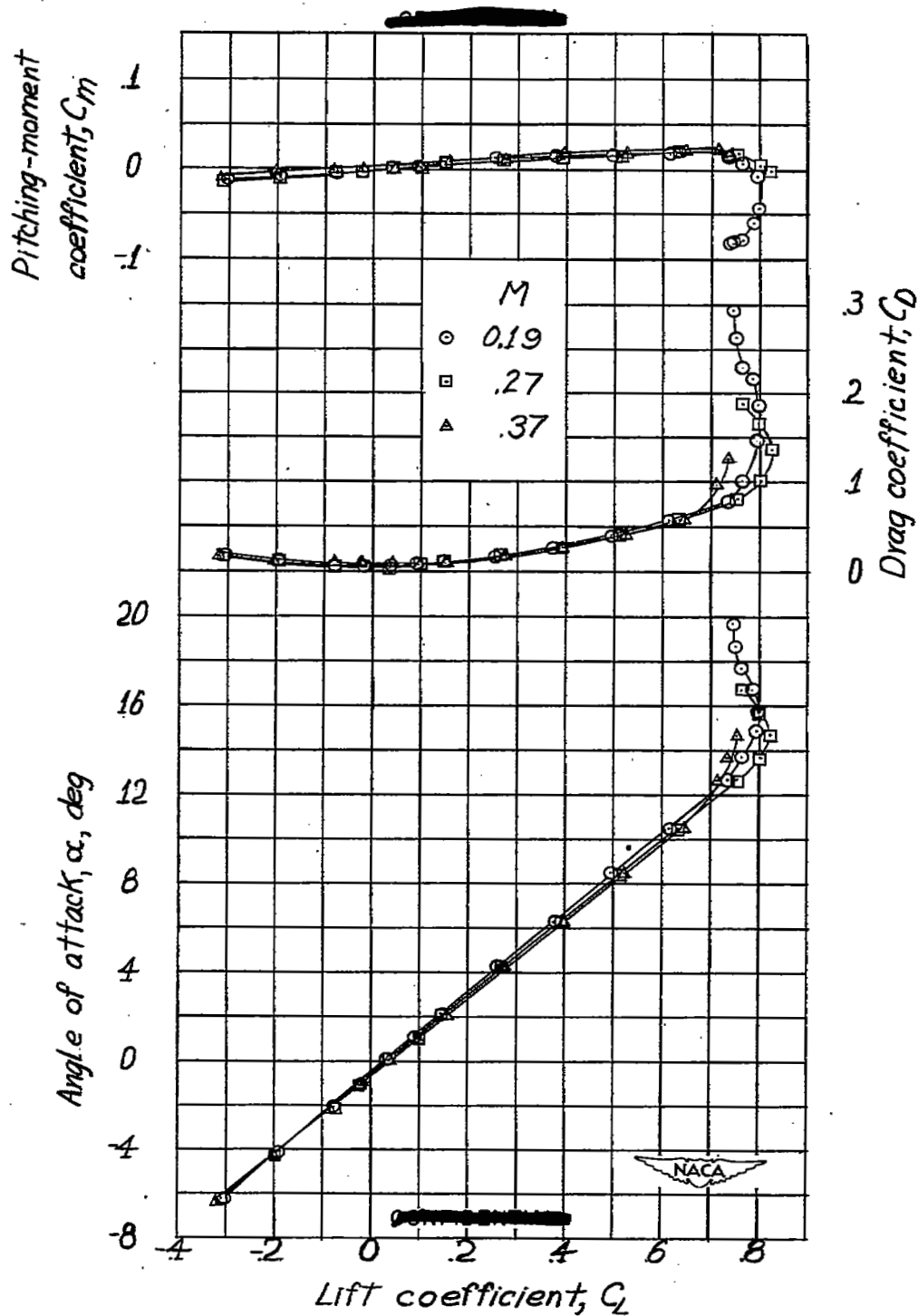


Figure 4.- Plain-wing aerodynamic characteristics of the unswept wing configuration for several Mach numbers.

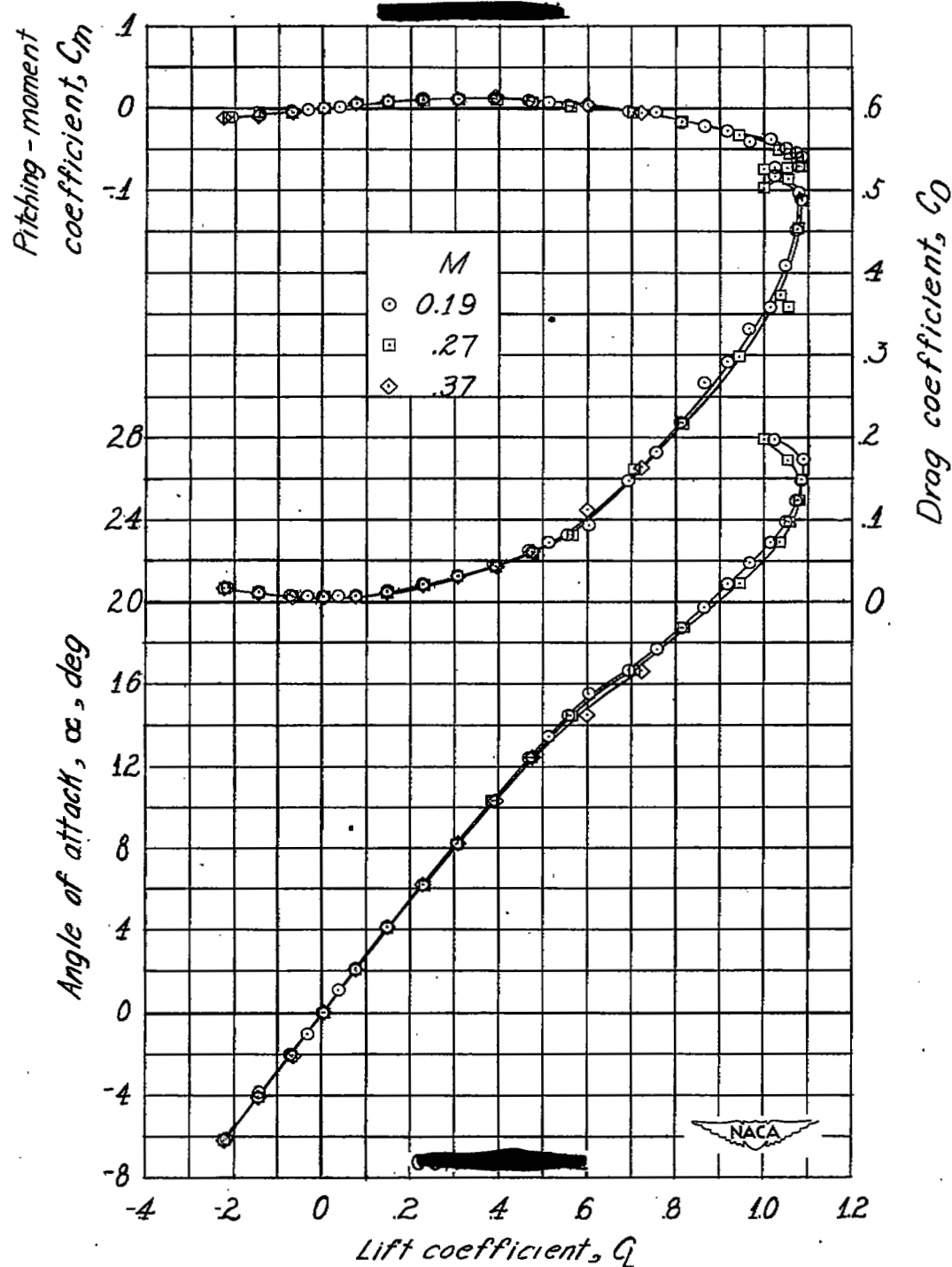


Figure 5.- Plain-wing aerodynamic characteristics of the 45° sweptback wing configuration for several Mach numbers.

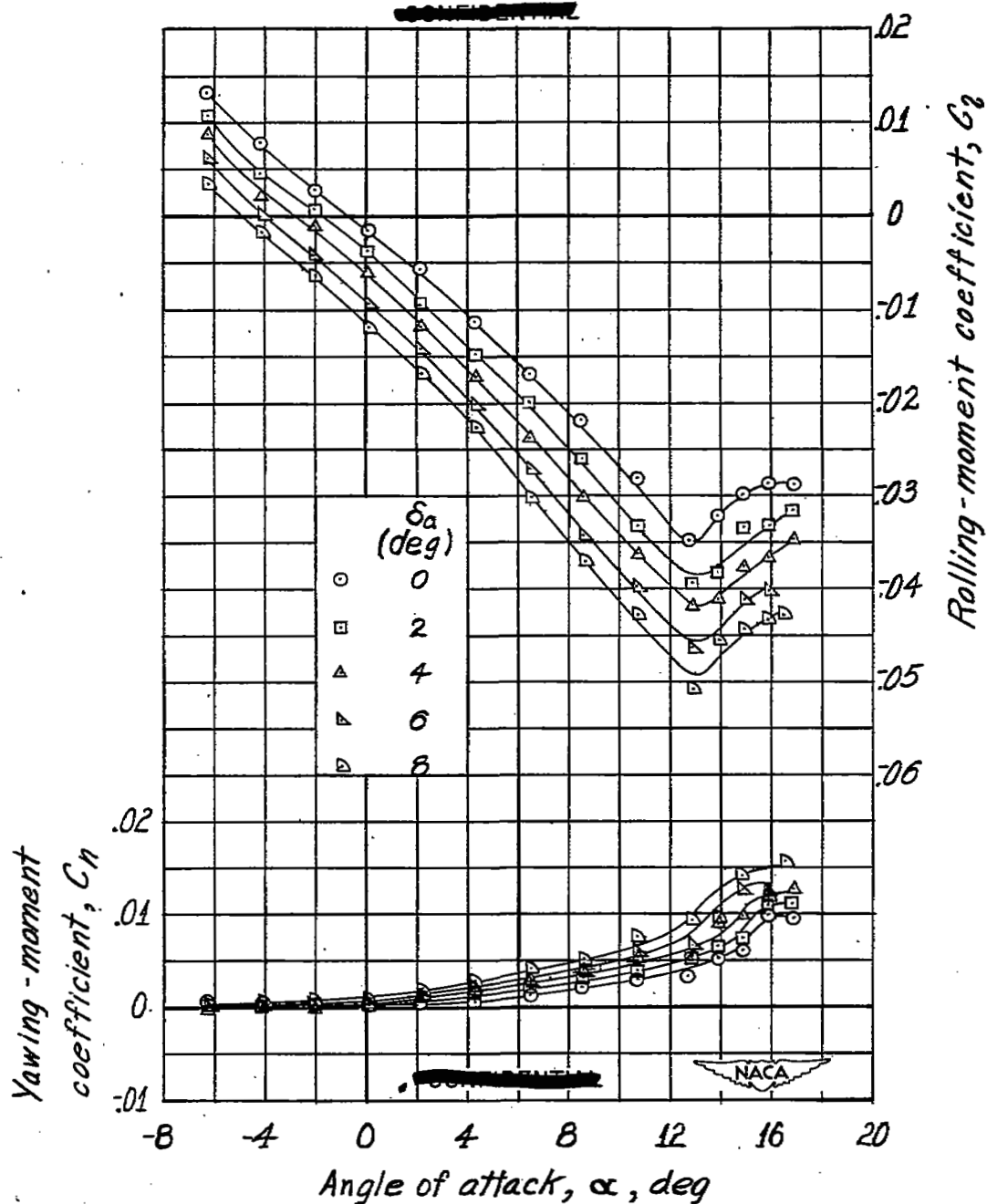


Figure 6.- Lateral control characteristics of unswept wing with large-chord wing-tip aileron at various deflections, fully extended.

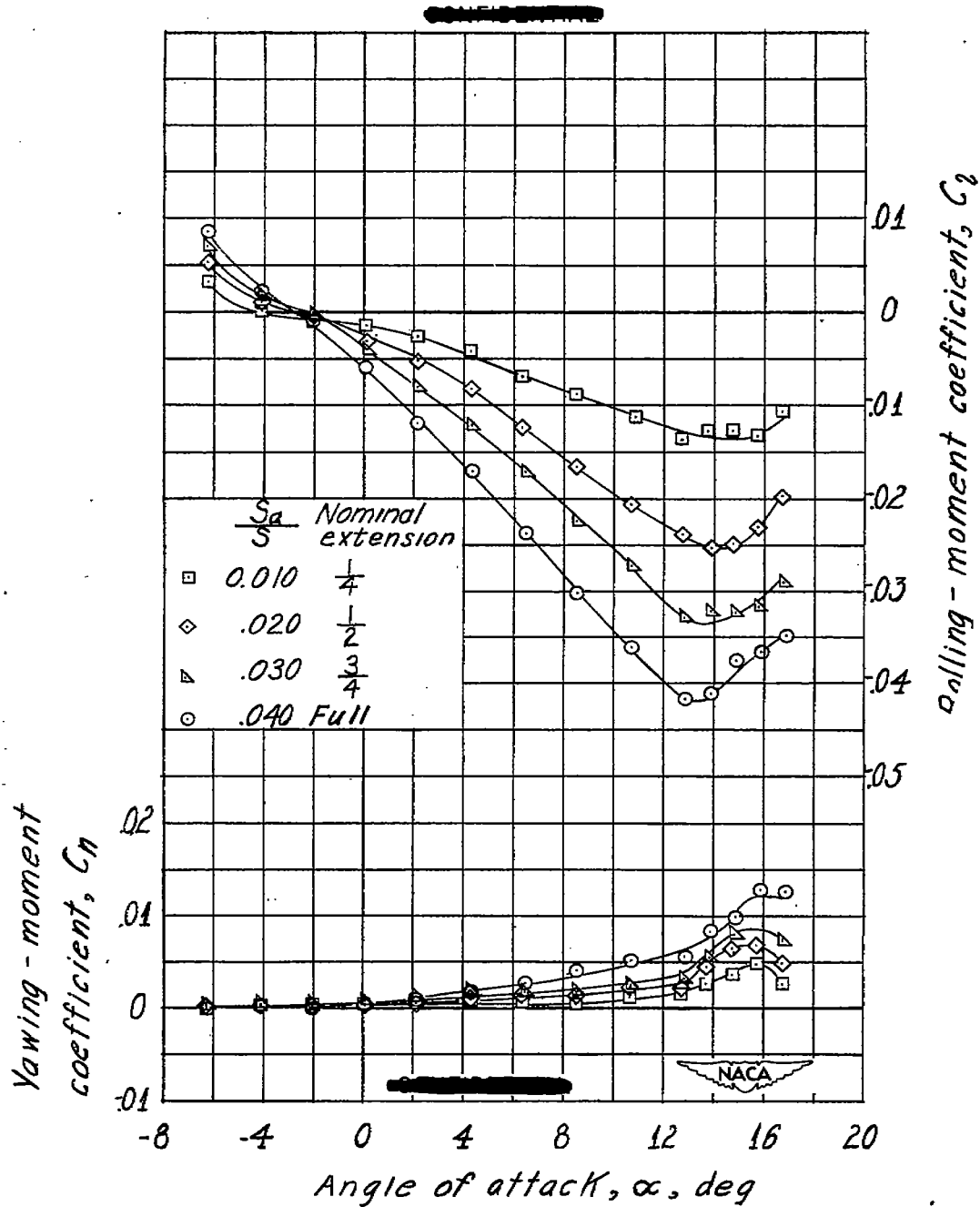
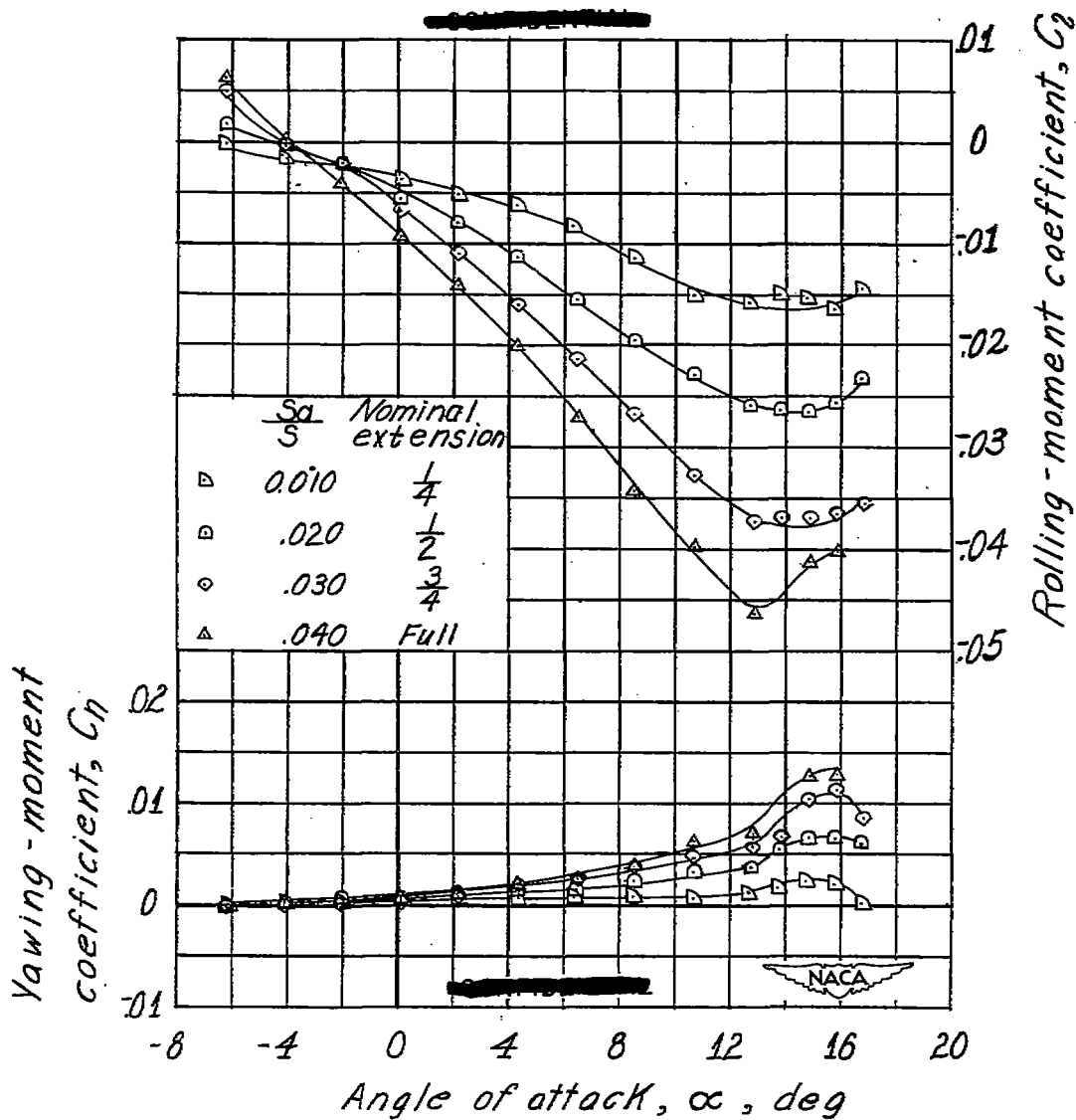
(a) $\delta_a = 4^\circ$.

Figure 7.- Lateral control characteristics of unswept wing with large-chord wing-tip aileron at various extensions.



(b) $\delta_a = -6^\circ$.

Figure 7.- Concluded.

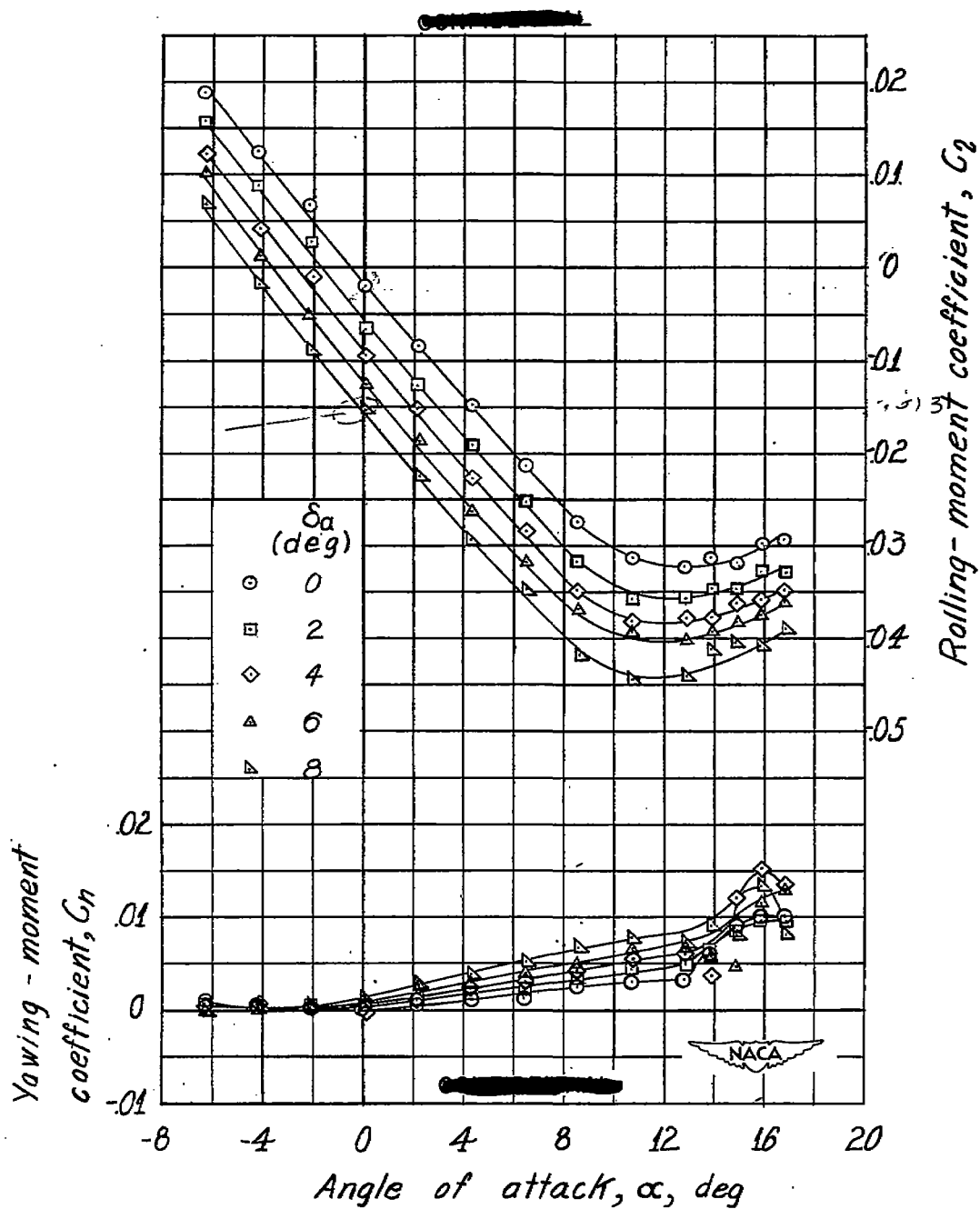
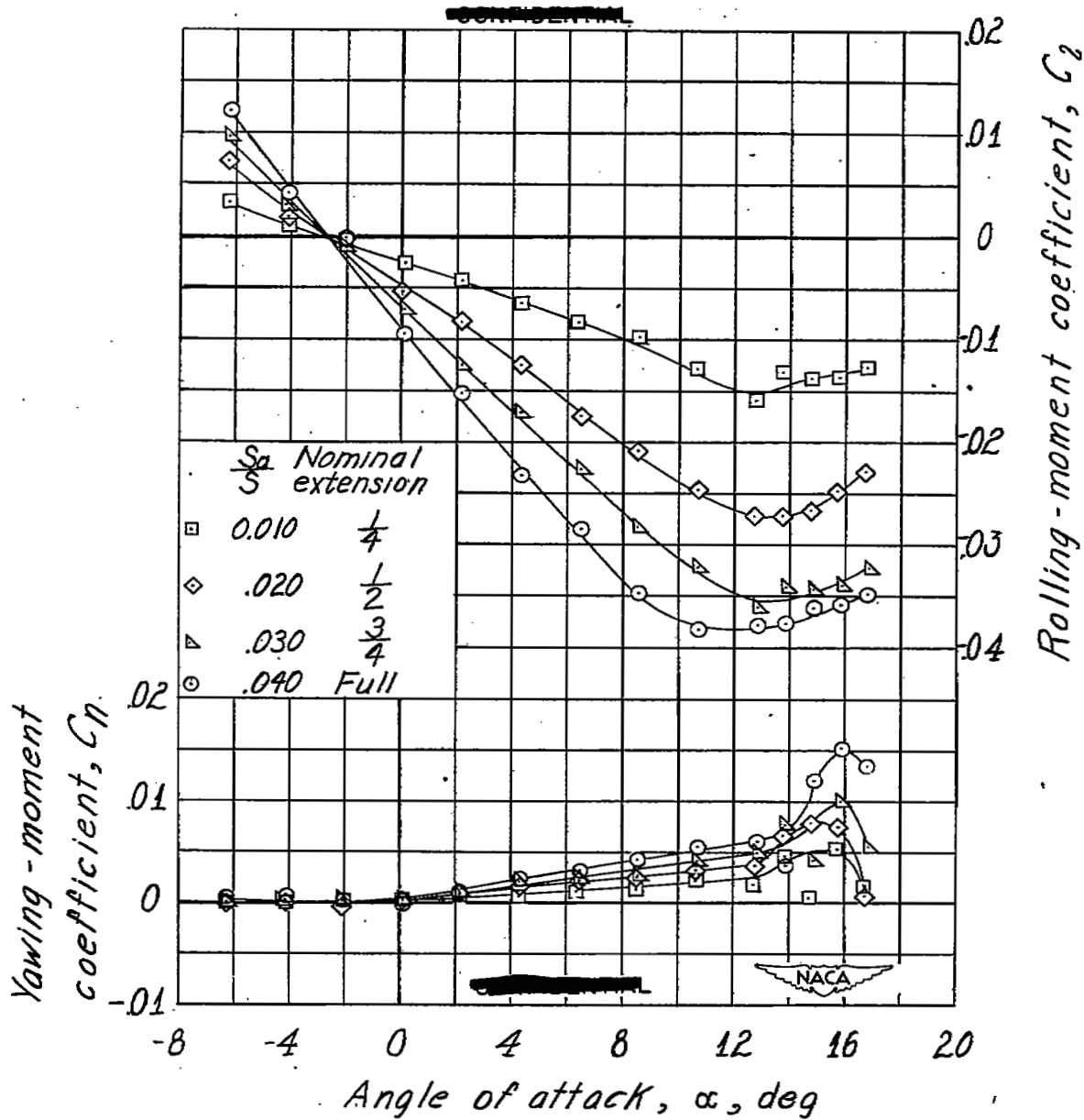


Figure 8.- Lateral control characteristics of unswept wing with triangular wing-tip aileron at various deflections, fully extended.



(a) $\delta_a = 14^\circ$.

Figure 9.- Lateral control characteristics of unswept wing with triangular wing-tip aileron at various extensions.

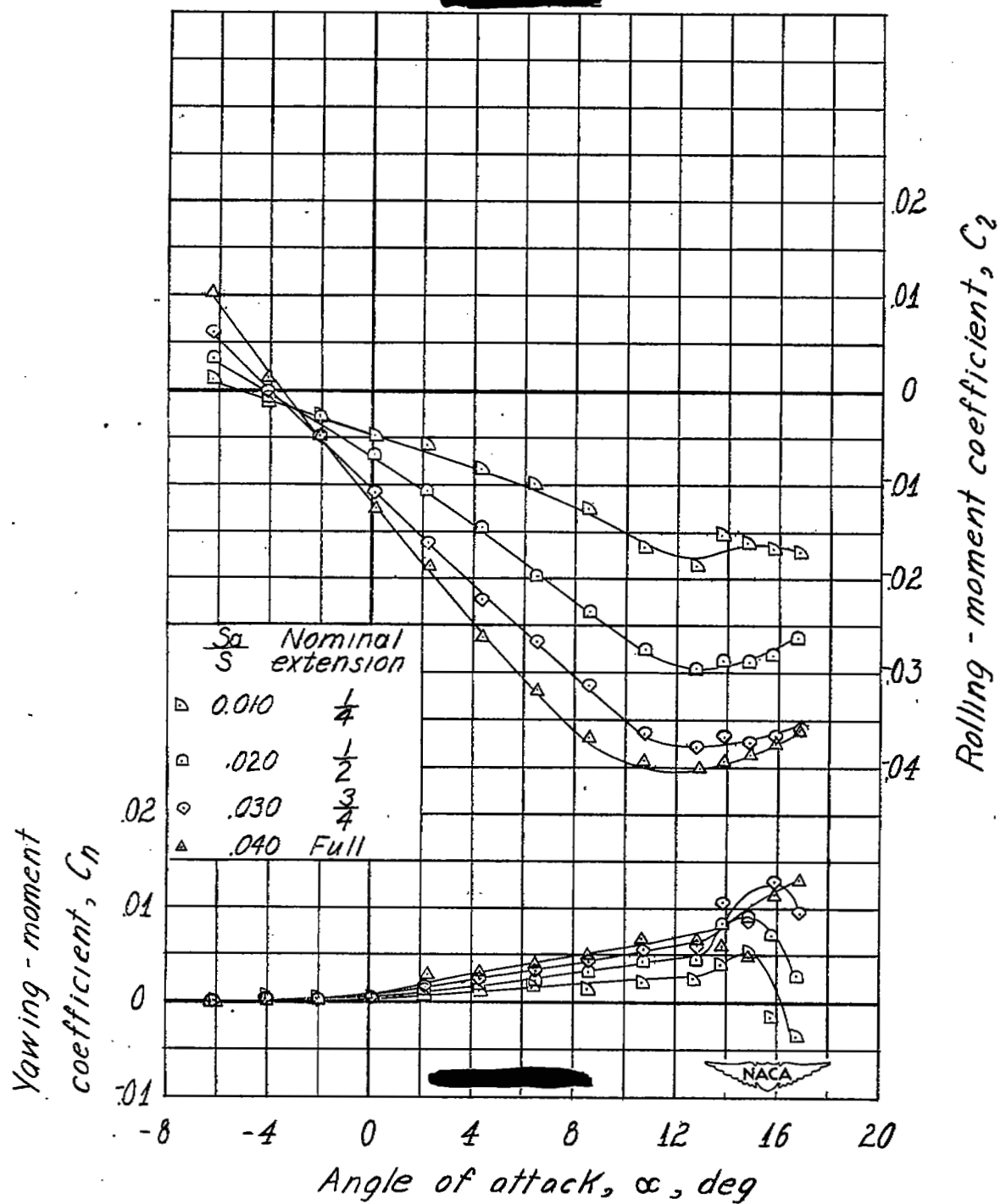
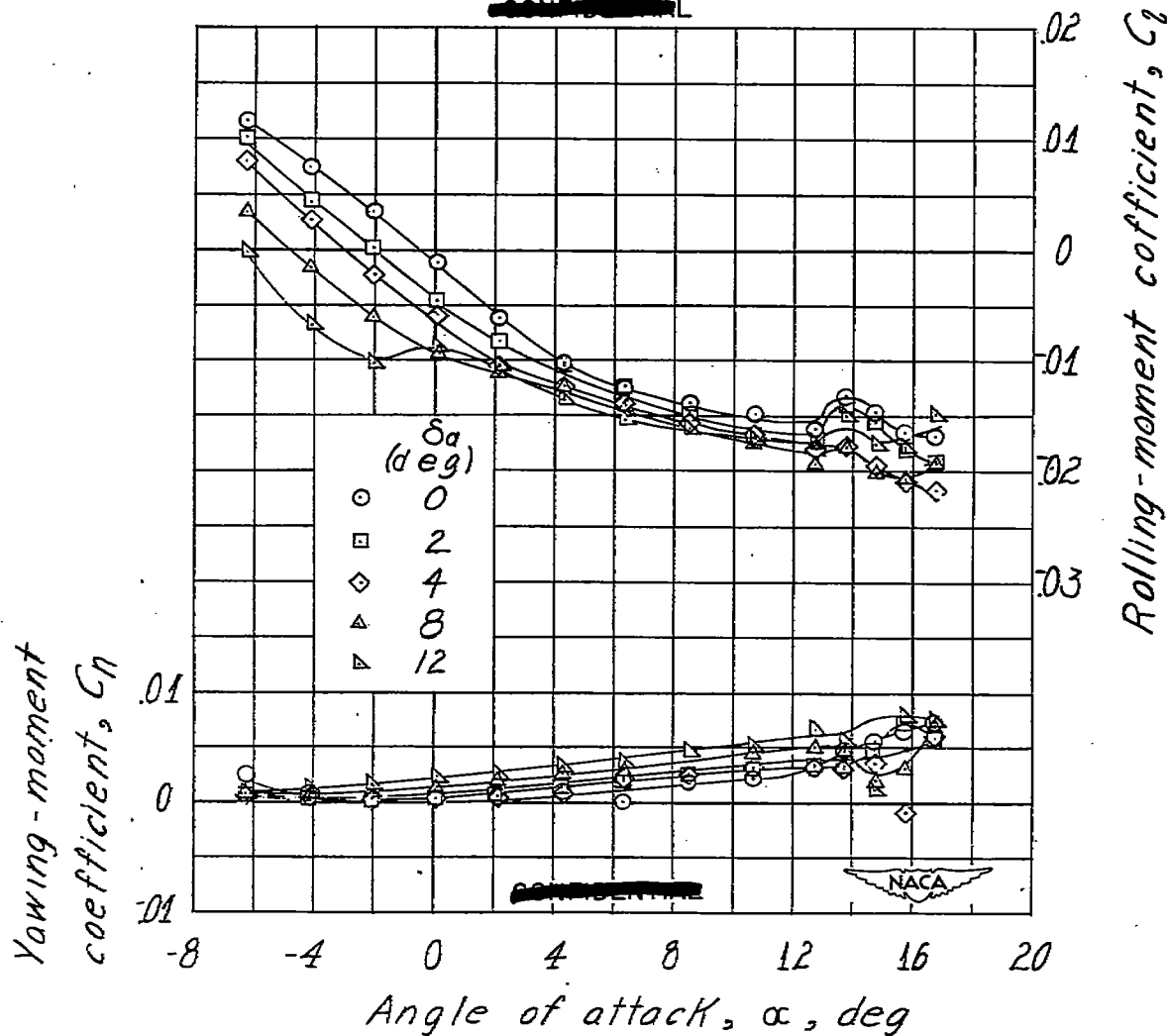
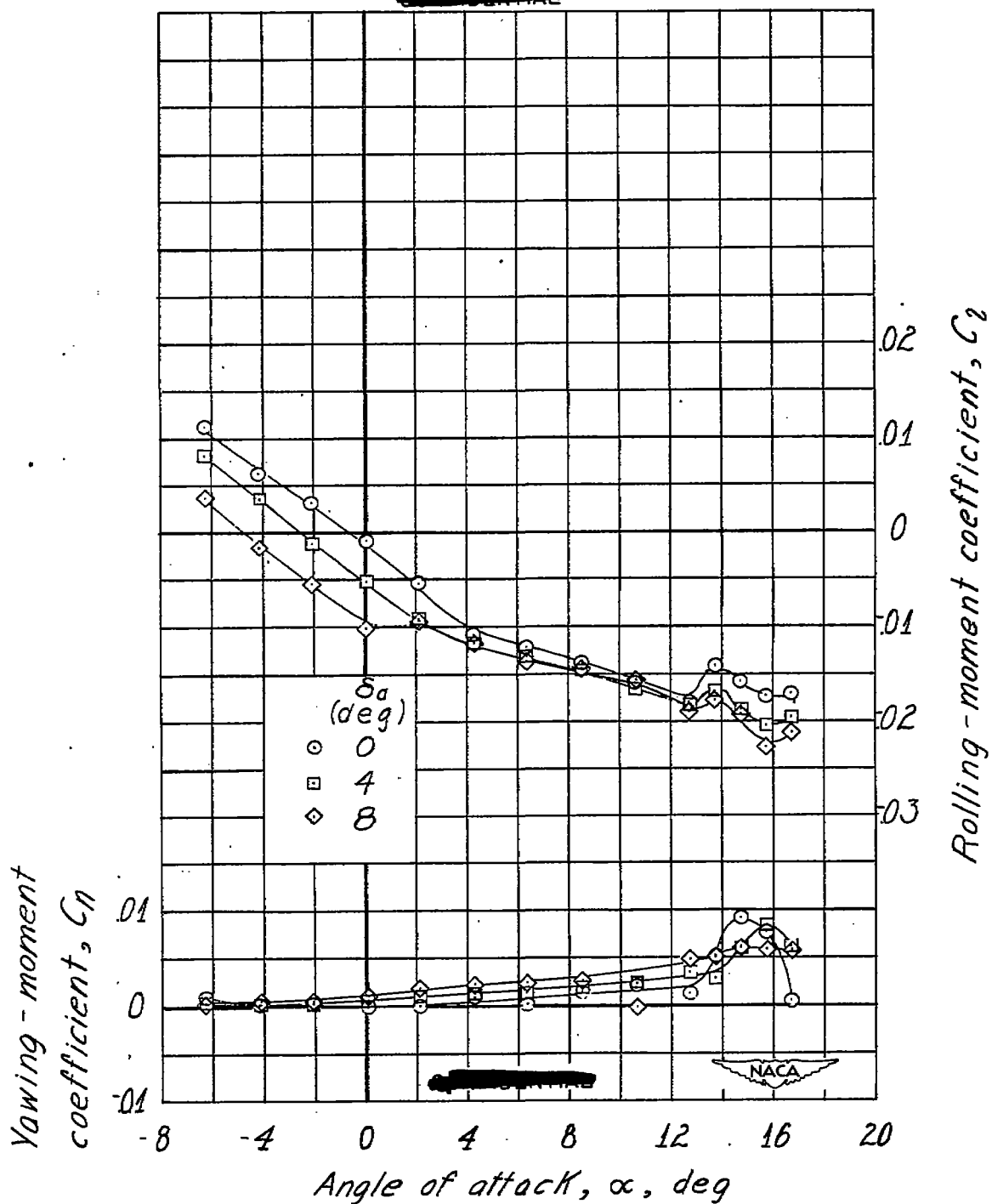
(b) $\delta_a = 6^\circ$.

Figure 9.- Concluded.



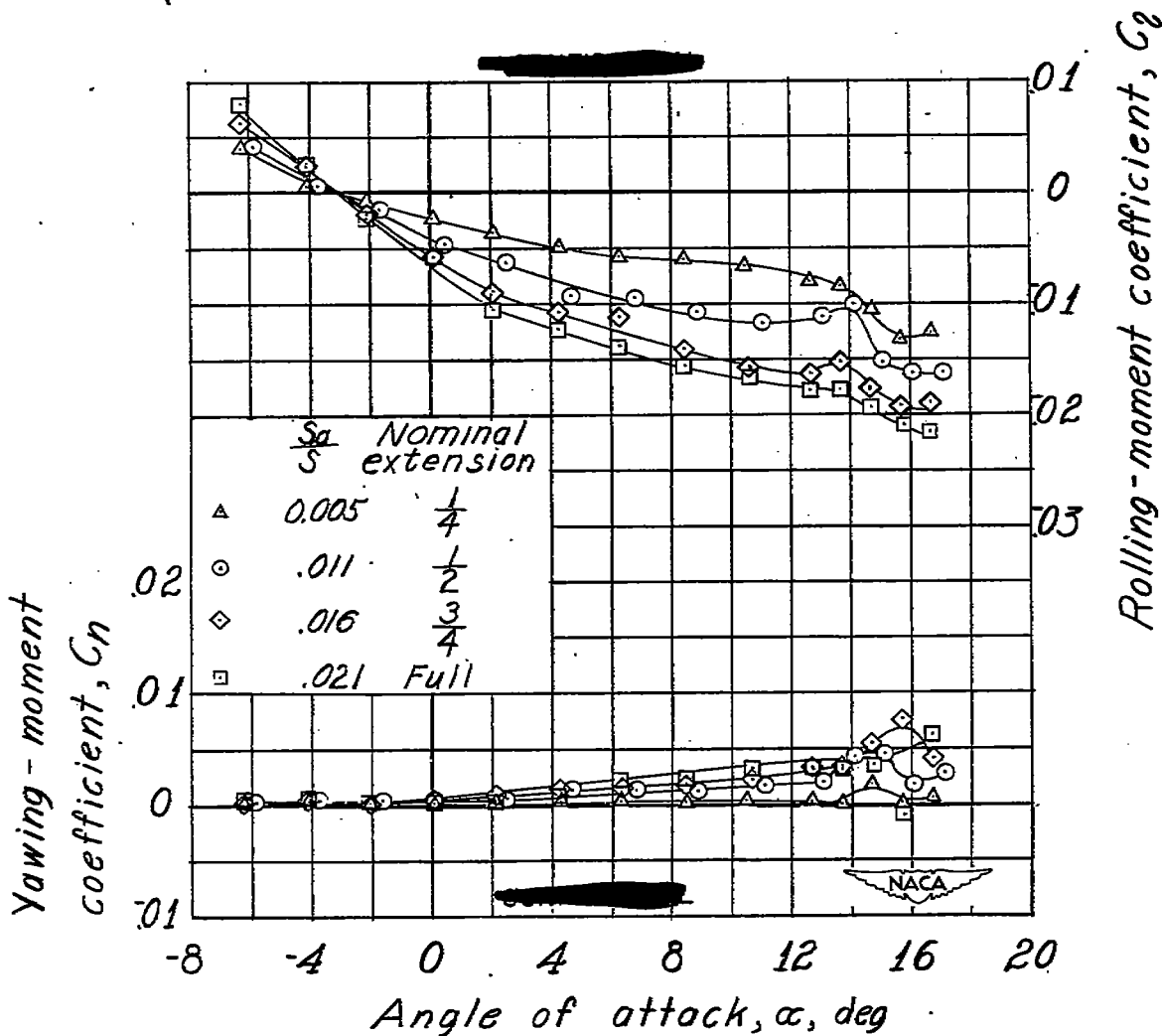
(a) Aileron pivoted at 0.50-chord station.

Figure 10.- Lateral control characteristics of unswept wing with small-chord wing-tip aileron at various deflections, fully extended.



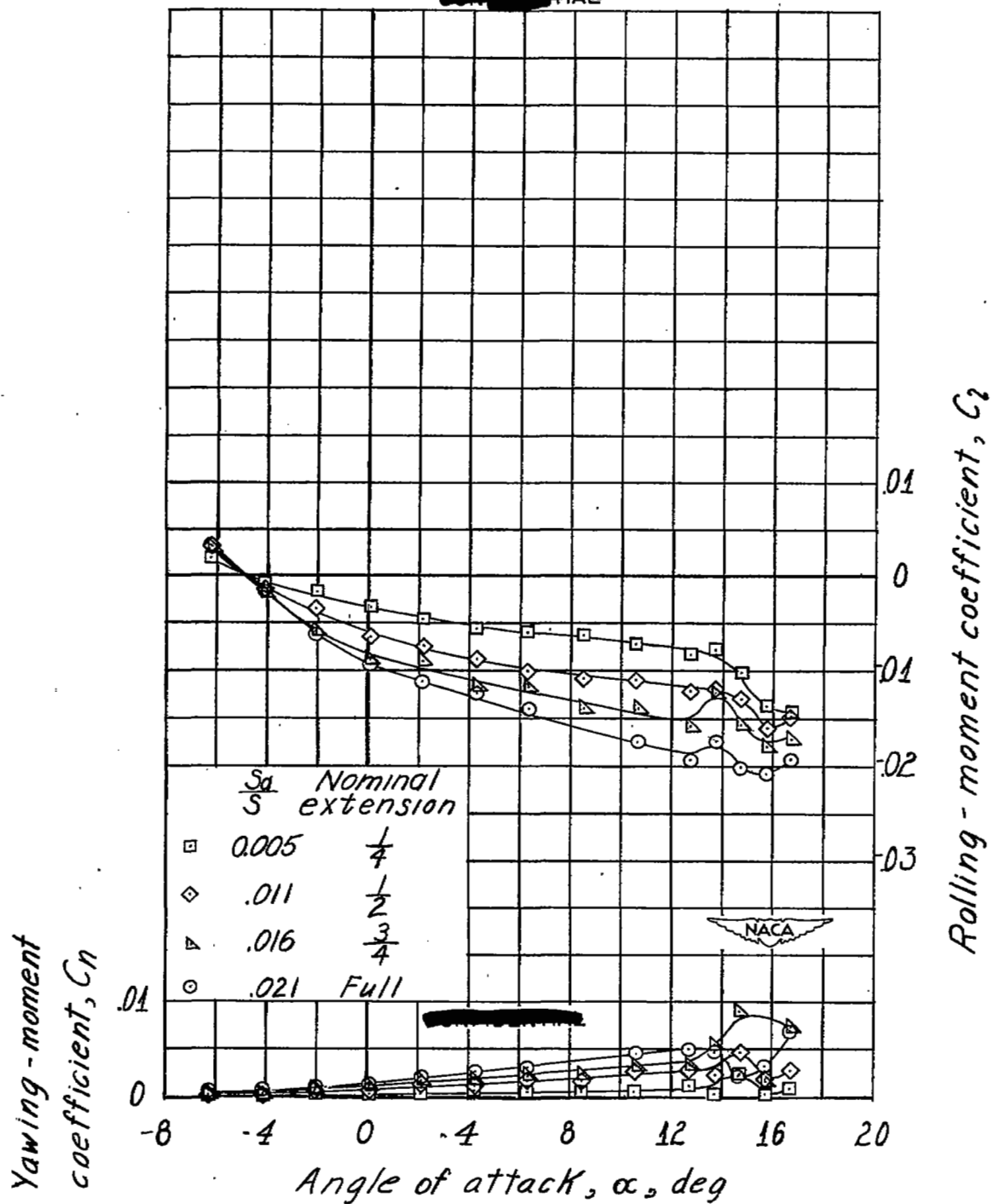
(b) Aileron pivoted at 0.267-chord station.

Figure 10.- Concluded.



(a) $\delta_a = 4^\circ$.

Figure 11.- Lateral control characteristics of unswept wing with short-chord wing-tip aileron at various extensions.



(b) $\delta_a = 8^\circ$.

Figure 11.- Concluded.

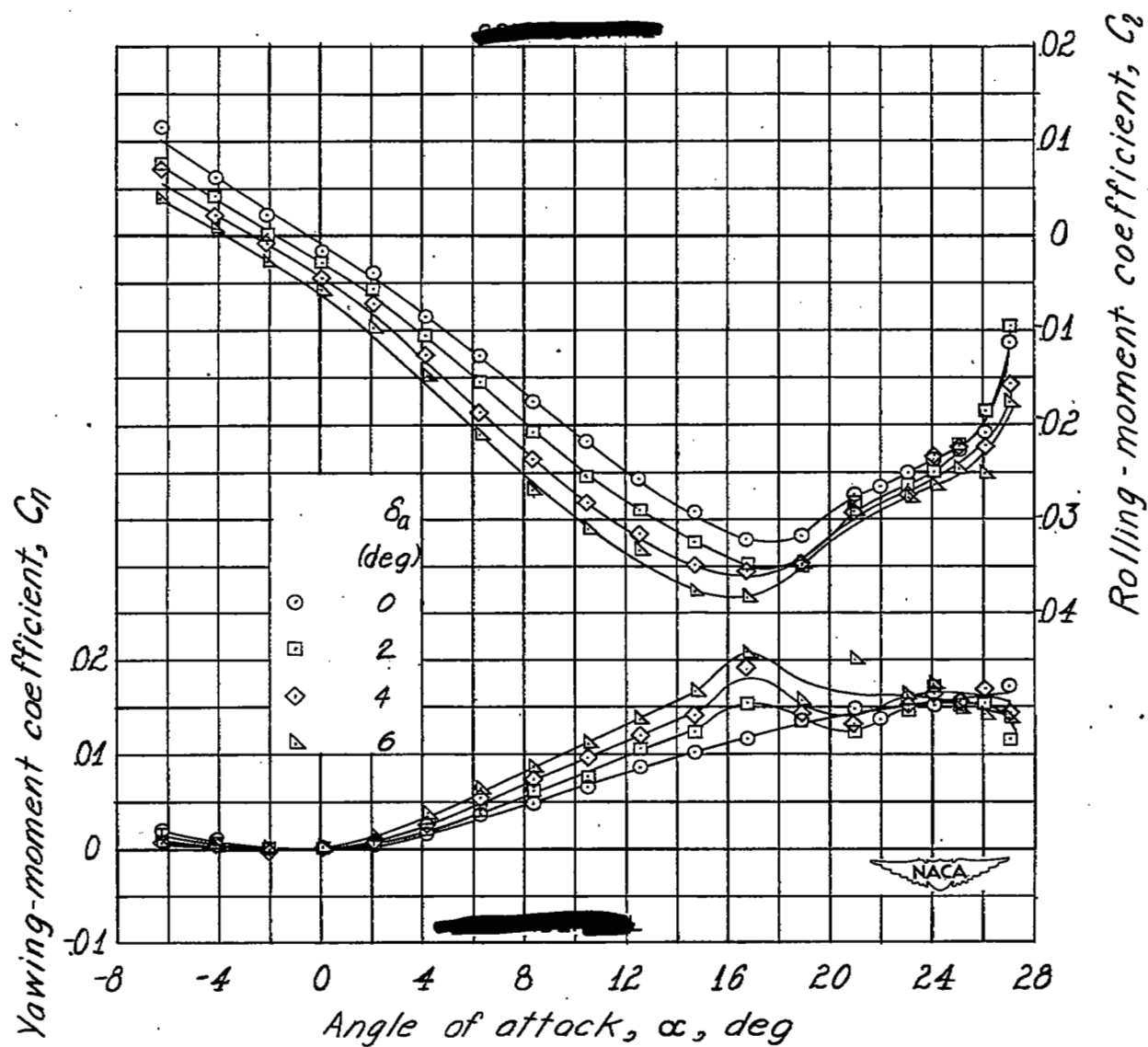


Figure 12.- Lateral control characteristics of 45° sweptback wing with large-chord wing-tip aileron at various deflections, fully extended.

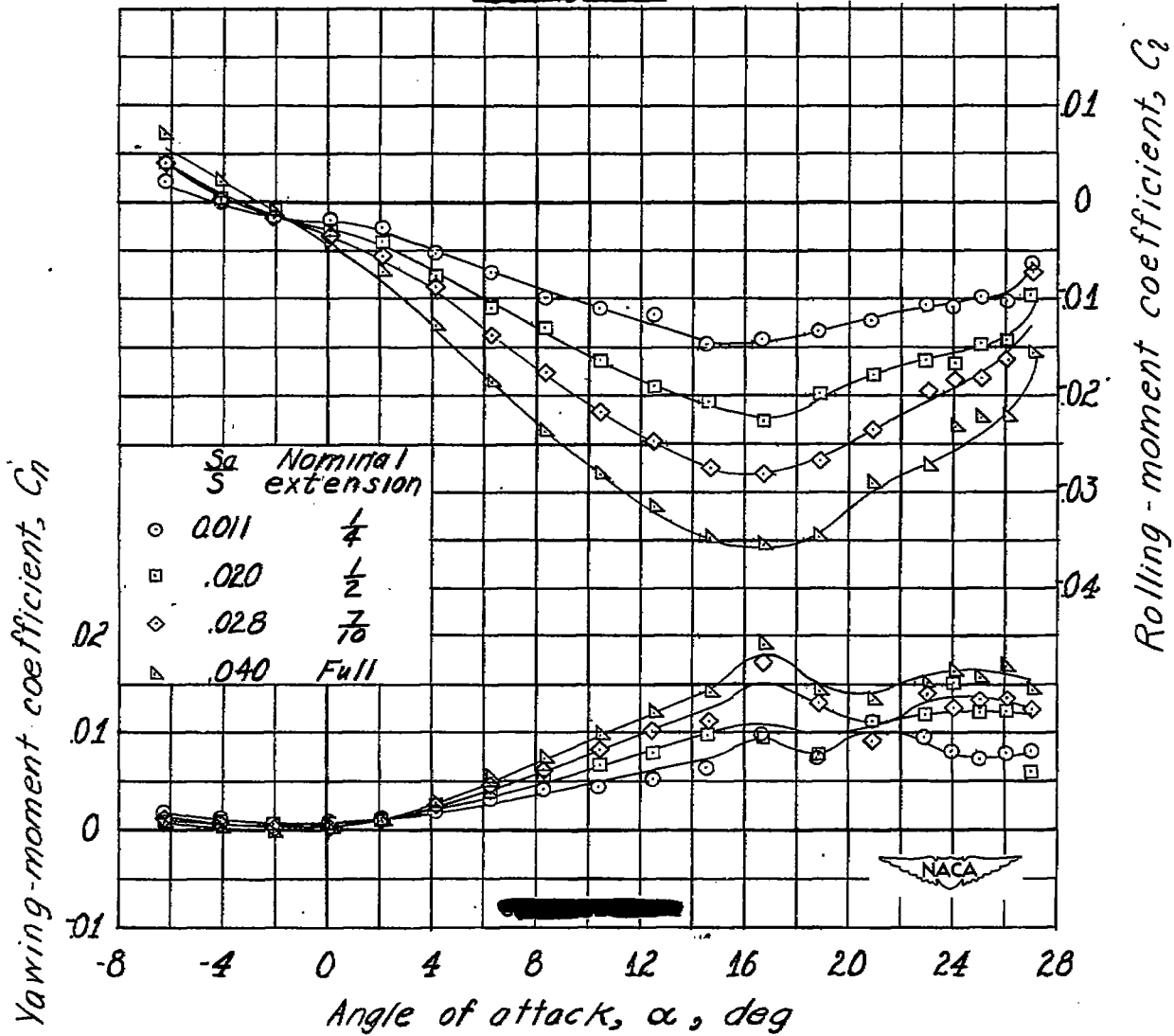


Figure 13.- Lateral control characteristics of 45° sweptback wing with large-chord wing-tip aileron at various extensions. $\delta_a = 4^\circ$.

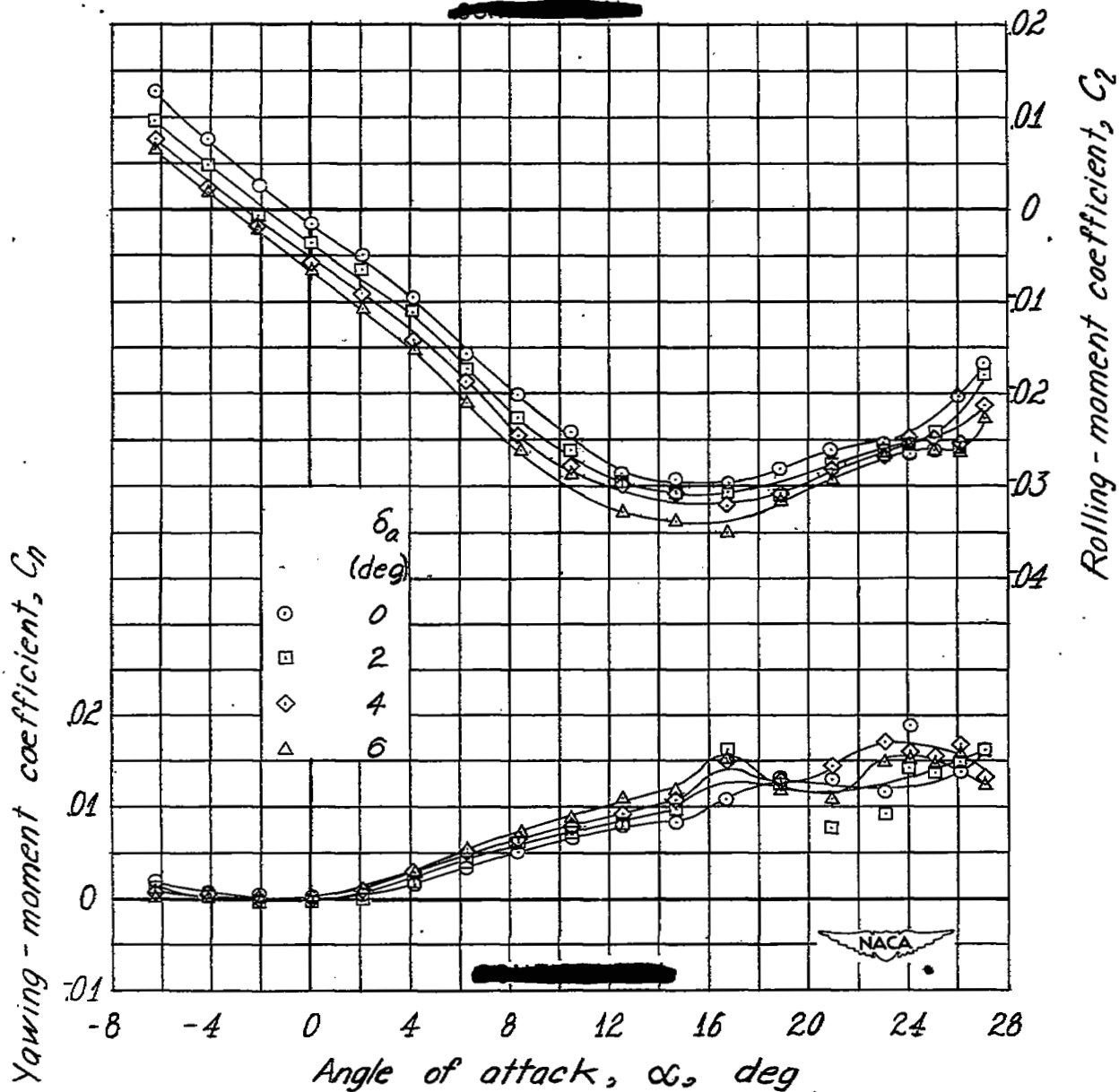


Figure 14.- Lateral control characteristics of 45° sweptback wing with triangular wing-tip aileron at various deflections, fully extended.

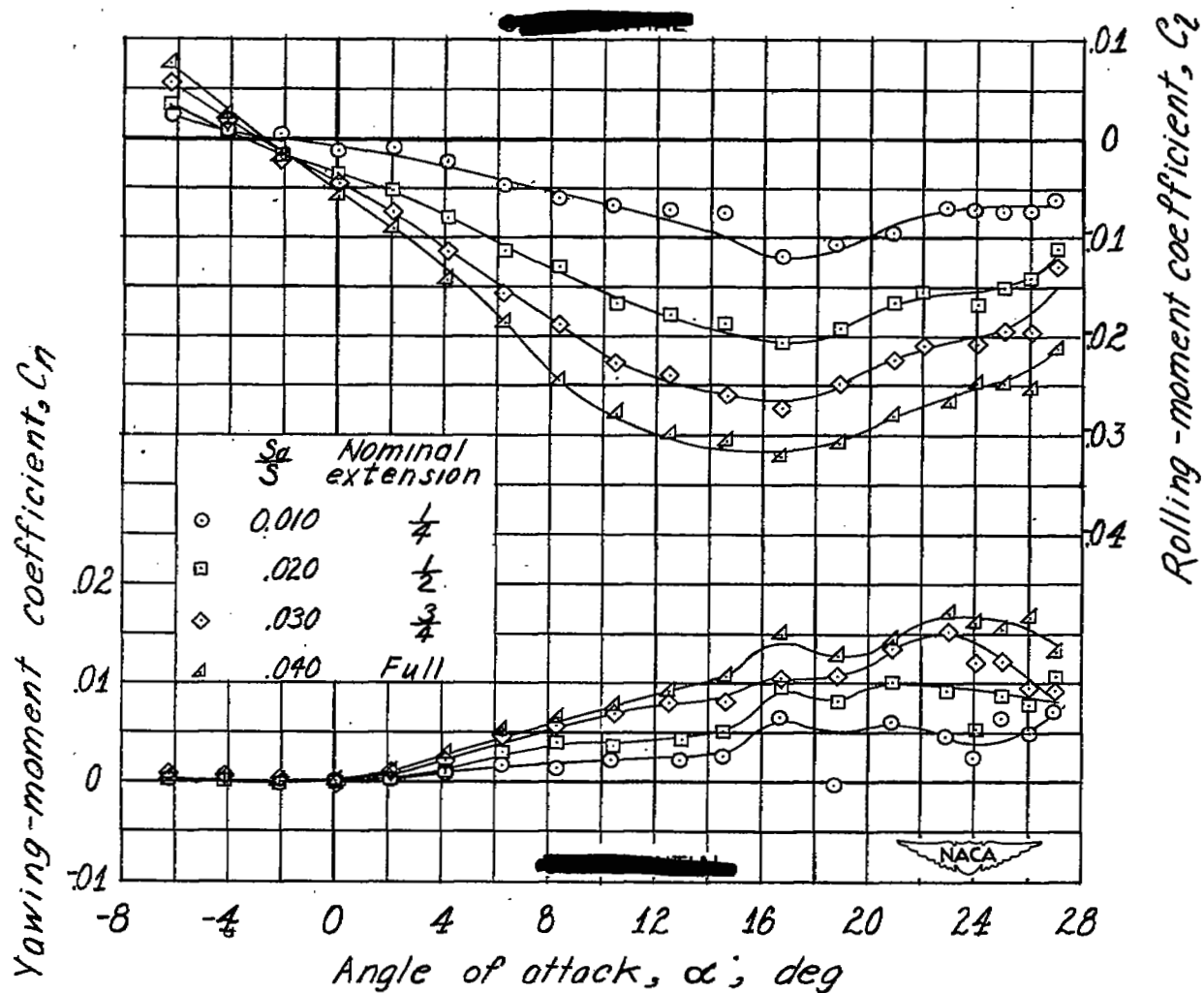


Figure 15.- Lateral control characteristics of 45° sweptback wing with triangular wing-tip aileron at various extensions. $\delta_a = 4^\circ$.

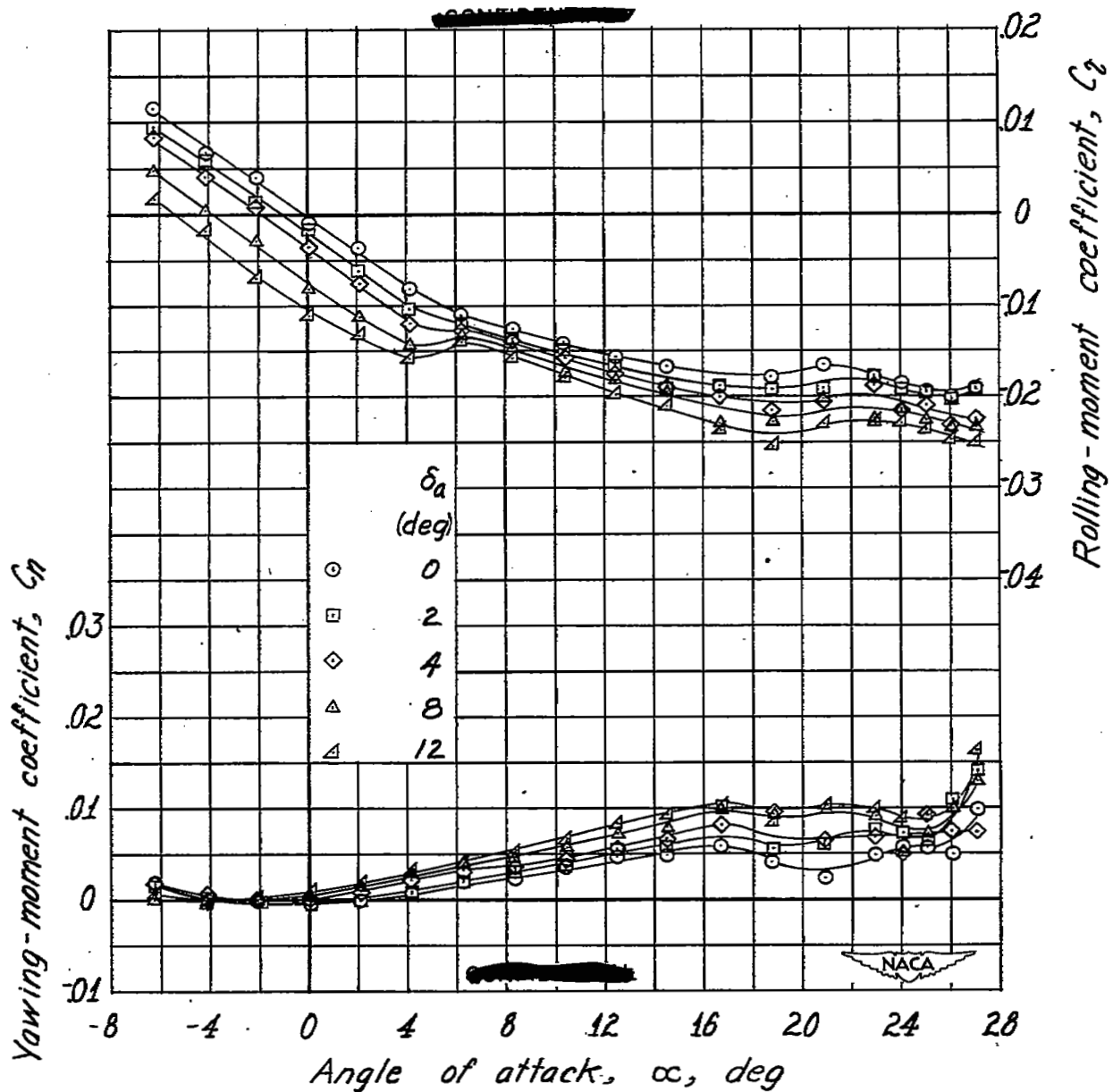


Figure 16.- Lateral control characteristics of 45° sweptback wing with short-chord wing-tip aileron at various deflections, fully extended.

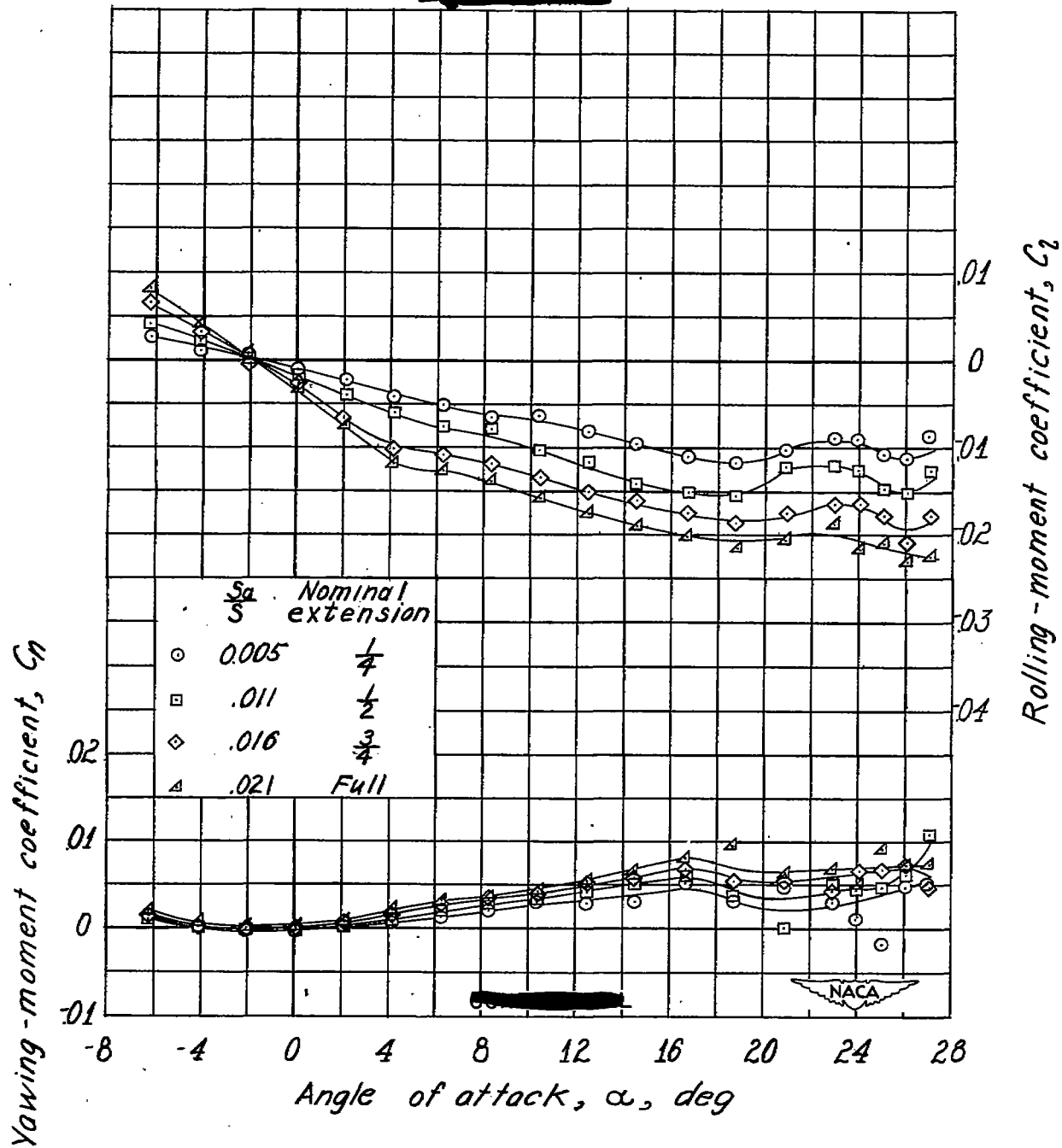
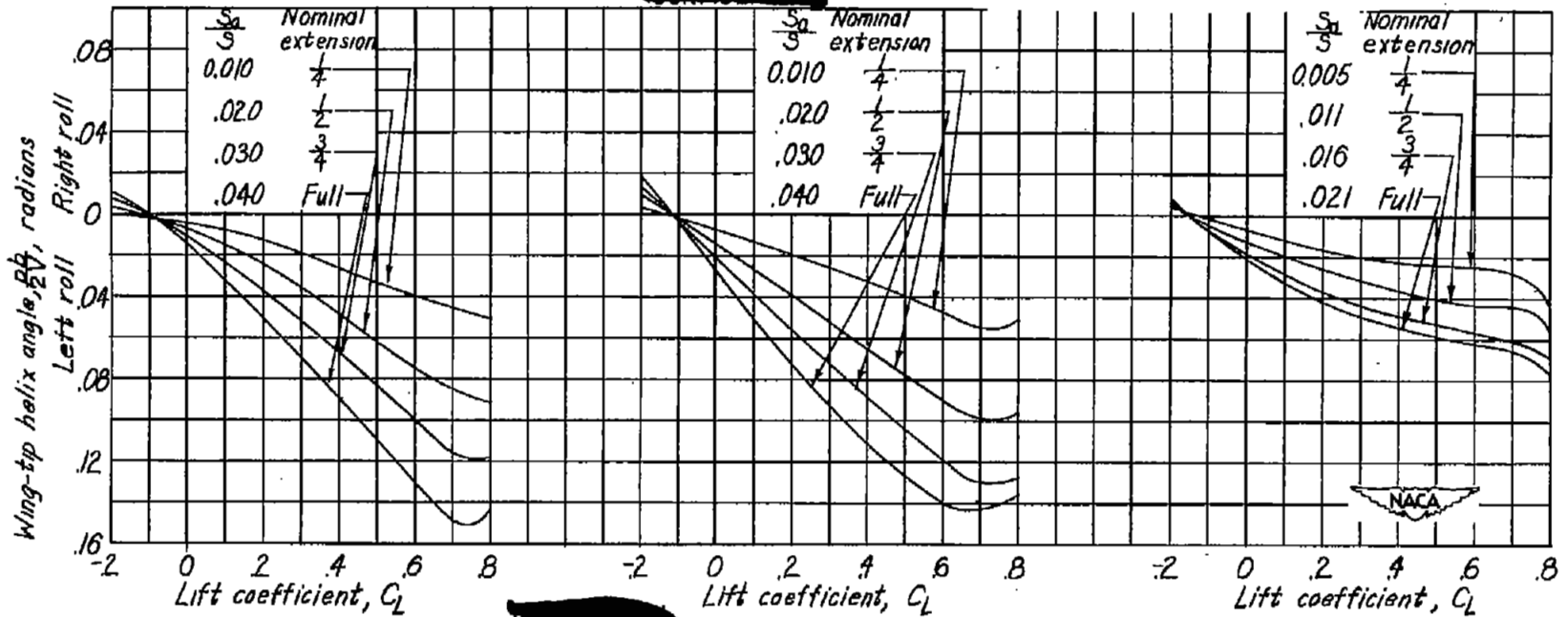


Figure 17.- Lateral control characteristics of 45° sweptback wing with short-chord wing-tip aileron at various extensions. $\delta_a = 4^\circ$.

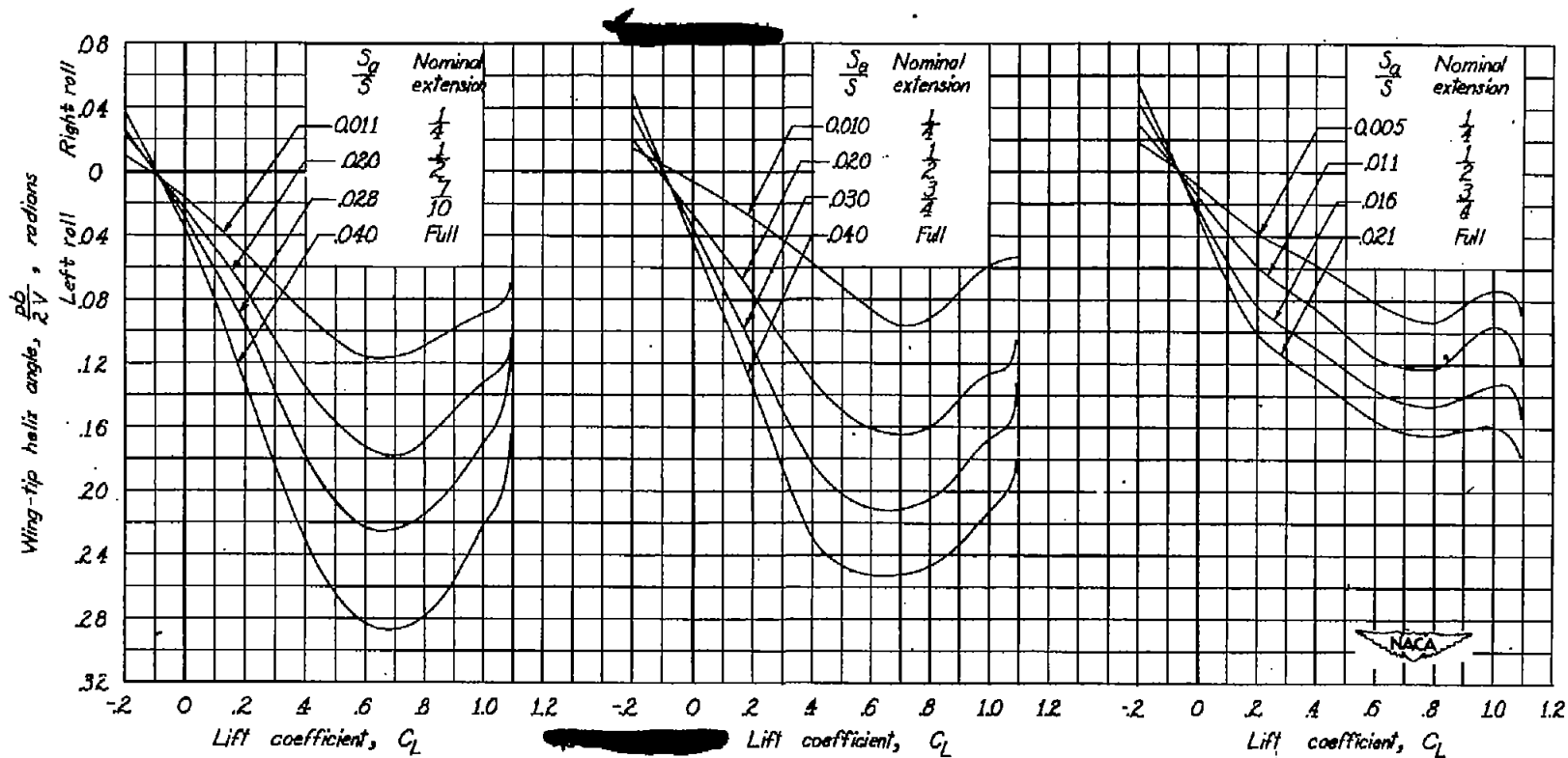


(a) Large-chord aileron.

(b) Triangular aileron.

(c) Short-chord aileron.

Figure 18.- Variation of wing-tip helix angle with lift coefficient for the unswept wing configuration with extensible wing-tip ailerons. $\delta_a = 4^\circ$.



(a) Large-chord aileron.

(b) Triangular aileron.

(c) Small-chord aileron.

Figure 19.- Variation of wing-tip helix angle with lift coefficient for the 45° sweptback wing with extensible wing-tip ailerons. $\delta_a = 4^\circ$.

NASA Technical Library



3 1176 01436 7719